Supporting Information

Examining the role of phosphorylation of p19^{INK4d} in its stability and ubiquitination using chemical protein synthesis

Muna Msallam[#], Hao Sun[#], Roman Meledin, Pauline Franz and Ashraf Brik*

Schulich Faculty of Chemistry, Technion-Israel Institute of Technology, Haifa 3200008, Israel.

Corresponding author: abrik@technion.ac.il

Table of Contents

1. Materials and methods

General methods

SPPS was carried out manually in syringes, equipped with Teflon filters, purchased from Torviq or by using an automated peptide synthesizer (CS336X, CSBIO). All the chemicals are analytical grade. N,N-dimethylformamide (DMF), dichloromethane (DCM), trifluoroacetic acid (TFA) and N,N-Diisopropylethylamine (DIEA) were purchased from Biolab. 4-Mercaptophenylacetic acid (MPAA), triisopropylsilane (TIS), dithiothreitol (DTT), and tert-Butylthiol (*t*-BuSH) were purchased from Sigma-Aldrich. Methyl 3-mercaptopropionate (MMP) was purchased from Acros Organics. 2,2'-Azobis[2-(2-imidazolin-2-yl)propane]dihydrochloride (VA044) was purchased from Wako Chemicals. Resins were purchased from CreoSalus, protected amino acids were purchased from GL Biochem and activating reagents [(2-(1H-benzotriazol-1-yl)-1,1,3,3-tetramethyluronium hexafluorophosphate (HBTU), hydroxybenzotriazole (HOBt), [(6-chlorobenzotriazol-1-yl)oxy- (dimethylamino)methylidene]-dimethylazanium hexafluorophosphate (HCTU), 1-[Bis(dimethylamino)methylene]-1H-1,2,3-triazolo[4,5-b]pyridinium 3-oxid hexafluorophosphate (HATU)] were purchased from Luxembourg Bio Technologies and GL Biochem. Analytical HPLC was performed on a Thermo instrument (Dionex Ultimate 3000) using analytical Xbridge (waters, BEH300 C4, 3.5 µm, 4.6 × 150 mm) and XSelect (waters, CSH C18, 3.5 µm, 4.6 × 150 mm) columns at a flow rate of 1.2 ml/min. Preparative and semi-preparative HPLC were performed on a Thermo instrument (Dionex Ultimate 3000) using Jupiter C4 (Phenomenex, 10µm, 250 × 21.2 mm) column and Jupiter C4 (Phenomenex, 10 µm, 300 Å, 250 × 10 mm) column, at flow rate of 15 and 4 mL/min respectively. All synthetic products were purified by HPLC and characterized by mass

spectrometry using LCQ Fleet Ion Trap (Thermo Scientific). All calculated masses have been reported as an average isotope composition. Buffer A: 0.1% TFA in water; buffer B: 0.1% TFA in acetonitrile.

List of the protected amino acids used in peptides synthesis

Fmoc-Gly-OH, Fmoc-Ala-OH, Fmoc-Val-OH, Fmoc-Leu-OH, Fmoc-Ile-OH, Fmoc-Phe-OH, Fmoc-Pro-OH, Fmoc-His(Trt)-OH, Fmoc-Asn(Trt)-OH, Fmoc-Gln(Trt)-OH, Fmoc-Arg(Pbf)-OH, Fmoc-Lys(Boc)-OH, Fmoc-Tyr(tBu)-OH, Fmoc-Ser(tBu)-OH, Fmoc-Thr(tBu)-OH, Fmoc-Asp(OtBu)-OH, Fmoc-Glu(OtBu)-OH, Fmoc-Trp(Boc)-OH, Fmoc-Met-OH, Fmoc-Cys(Acm)-OH, Fmoc-Cys(Trt)-OH, Fmoc-Ser(PO_3BzlH)-OH, Boc-Cys(Trt)-OH, Boc-Thz-OH, Boc-Leu-OH, Fmoc-Leu-Thr(ψMe,MePro)-OH, Fmoc-Lys(Boc)-Thr(ψMe,MePro)-OH, Fmoc-Asp(OtBu)-(Dmb)Gly-OH, Fmoc-Leu-Ser(ψMe,MePro)-OH, Fmoc-Glu(OtBu)-Ser(psiMe,Mepro)-OH, Fmoc-Val-Ser(psiMe,Mepro)-OH, Fmoc-Asp(OtBu)-Thr(psiMe,Mepro)-OH, Fmoc-Gly-Thr(psiMe,Mepro)-OH, Fmoc-Ser(tBu)-Thr(psiMe,Mepro)-OH.

2. Synthesis of fragment 1, Cys-p19^{INK4d}(109-166)

The synthesis was carried out on Knorr Resin (0.26 mmol/g, 0.2 mmol scale). The amino acids were coupled by standard Fmoc-SPPS on the synthesizer to complete the peptide synthesis. Pseudoproline dipeptides, Fmoc-Leu-Thr(psiMe,Mepro)-OH, Fmoc-Glu(OtBu)-Ser(psiMe,Mepro)-OH, Fmoc-Val-Ser(psiMe,Mepro)-OH were coupled manually using dipeptide (2.5 equiv), HATU (2.5 equiv) and DIEA (5 equiv) for 90 min at positions Leu140-Thr141, Glu129-Ser130, Val123-Ser124, respectively. Peptide cleavage was carried out using the cocktail of TFA: triisopropylsilane: water (95: 2.5: 2.5). Progress of the reaction was monitored by analytical HPLC with a gradient of 0-60% B in 30 min (A: 0.1% TFA in water; B: 0.1% TFA in acetonitrile). The peptide was purified using a preparative column with the same gradient to obtain fragment **1**, Cys-p19^{INK4d}(109-166) (22.4 % yield, 284 mg from 0.2 mmol).

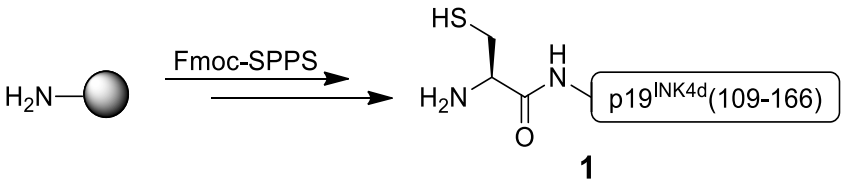

1

Scheme S1. Synthetic steps for fragment **1**, Cys-p19^{INK4d}(109-166).

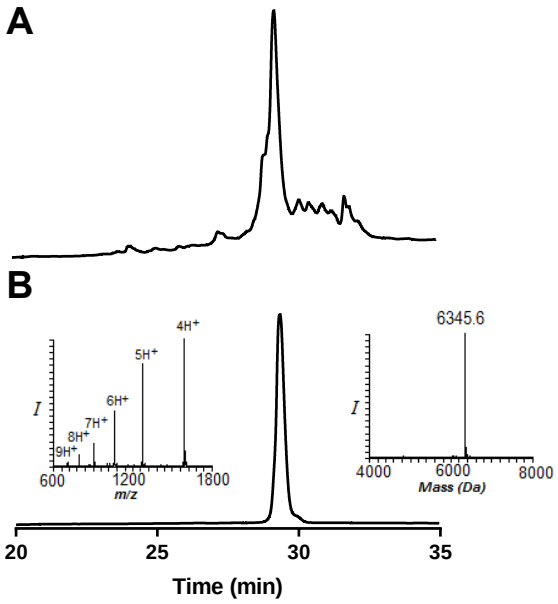

Figure S1. (A) HPLC of crude fragment **1**, Cys-p19 ^{INK4d}(109-166). (B) HPLC and mass analysis of purified fragment **1**, Cys-p19 ^{INK4d}(109-166) with observed mass of 6345.6 ± 0.4 Da (calculated 6345.3 Da).

3. Synthesis of fragment 2, Thz-p19^{INK4d}(56-107)(S^{P}66 & S^{P}76)-MMP

The synthesis was carried out on Knorr Resin (0.26 mmol/g, 0.2 mmol scale). Fmoc-MeDbz (4 equiv) was coupled to the resin using HATU (4 equiv), DIEA (8 equiv) for 90 min. Pseudoproline dipeptides, Fmoc-Asp(OtBu)-(Dmb)Gly-OH, Fmoc-Asp(OtBu)-Thr(psiMe,Mepro)-OH and Fmoc-Gly-Thr(psiMe,Mepro)-OH were coupled manually using dipeptide (2.5 equiv), HATU (2.5 equiv) and DIEA (5 equiv) for 90 min at positions Asp104-Gly105, Asp88-Thr89, Gly74-Thr75, respectively. Fmoc-Ser(PO_3BzlH)-OH (2.5 equiv) was coupled manually using HATU (2.5 equiv) and DIEA (5 equiv) for 90 min. The other amino acids were coupled using standard Fmoc-SPPS on a peptide synthesizer. After completion of SPPS, the peptide on the resin (0.1 mmol) was treated with p-nitrophenyl chloroformate (100 mg, 5 equiv) in 4 ml dry DCM for 30 min (3 cycles), and was washed with DCM and DMF, followed by treatment in 4 ml of 0.5 M DIEA in DMF for 10 min (3 cycles). The peptide cleavage was carried using the cocktail of TFA: triisopropylsilane: EDT: water (94: 1: 2.5: 2.5). The crude peptide (25 mg) was dissolved in 6 M Gn·HCl/200 mM phosphate buffer (pH 7.0, 1.5 ml) containing MMP (200 equiv, 95 μL), and incubated at 37 ºC for 1 h. The progress of the reaction was monitored, and the product was purified using HPLC with a gradient of 0-60% B in 30 min to obtain fragment **2**, Thz-p19^{INK4d}(56-107)(S^{P}66 & S^{P}76)-MMP in 19.4 % isolated yield (221 mg from 0.2 mmol).

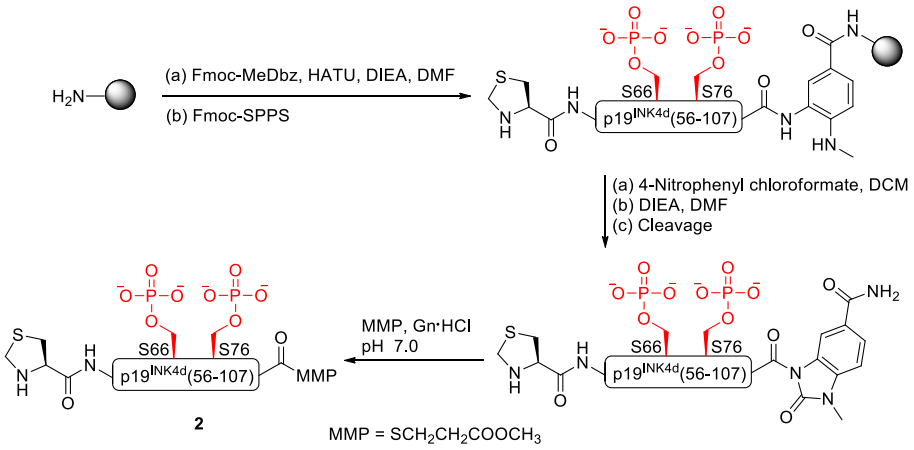

Scheme S2. Synthetic steps for fragment **2**, Thz-p19^{INK4d}(56-107)(S^{P}66 & S^{P}76)-MMP.

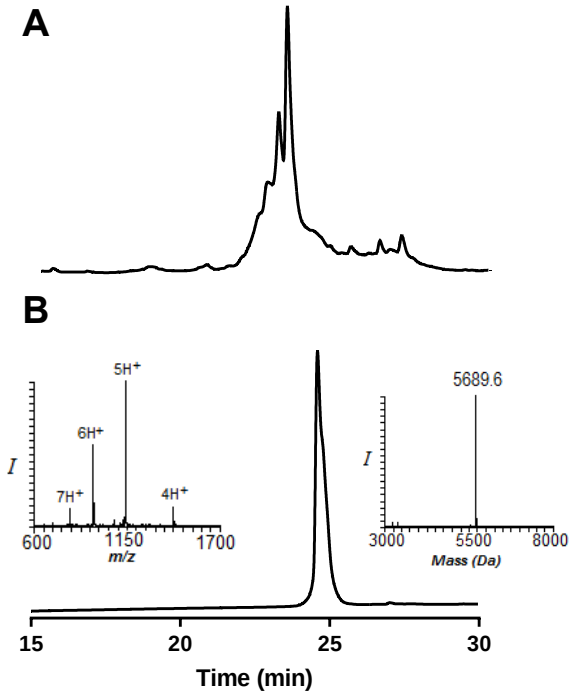

Figure S2. (A) HPLC of crude Thz-p19^{INK4d}(56-107)(S^{P}66 & S^{P}76)-MeDbz. (B) HPLC and mass analysis of purified fragment **2**, Thz-p19^{INK4d}(56-107)(S^{P}66 & S^{P}76)-MMP with observed mass of 5689.6 ± 0.3 Da (calculated 5688.0 Da).

4. Synthesis of Thz-p19^{INK4d}(56-107)-MMP

Synthesis, analysis, and purification were carried out in the same manner as described for fragment **2** (Scheme S2) to obtain fragment **6**, Thz-p19^{INK4d}(56-107)-MMP in 24.3 % isolated yield (269 mg, from 0.2 mmol).

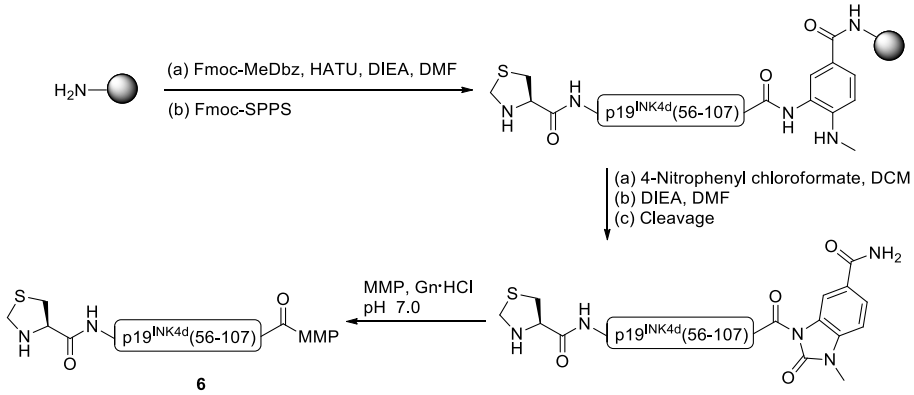

Scheme S3. Synthetic steps for Thz-p19^{INK4d}(56-107)-MMP.

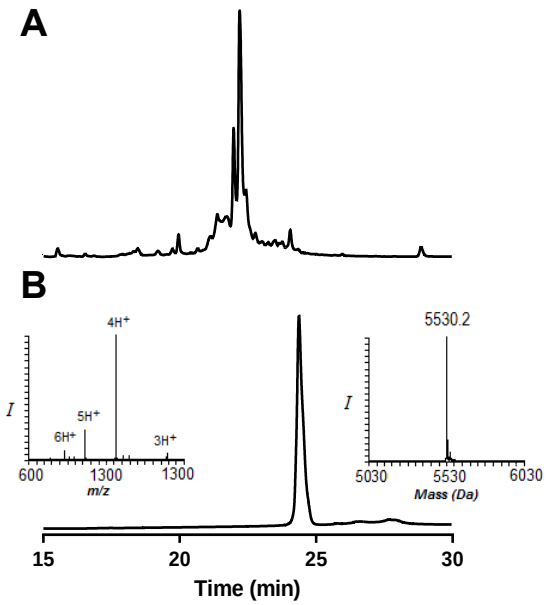

Figure S3. (A) HPLC of crude Thz-p19^{INK4d}(56-107)-MeDbz. (B) HPLC and mass analysis of purified fragment **6**, Thz-p19^{INK4d}(56-107)-MMP with observed mass of 5530.2 ± 0.2 Da (calculated 5530.0 Da).

5. Synthesis of Thz-p19^{INK4d}(56-107)(S^{P}66)-MMP

Synthesis, analysis, and purification were carried out as in the same manner described for fragment **2** (Scheme S2) to obtain the fragment **7**, Thz-p19^{INK4d}(56-107)(S^{P}66)-MMP in 22.9 % yield (257 mg from 0.2 mmol).

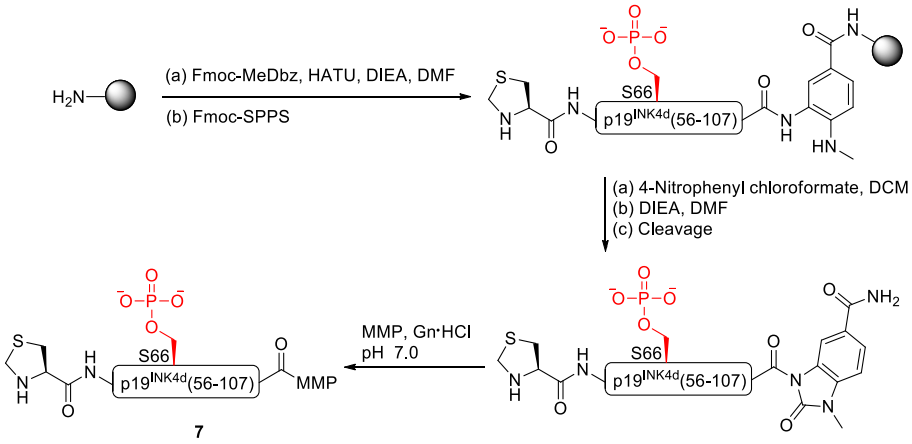

Scheme S4. Synthetic steps for Thz-p19^{INK4d}(56-107)(S^{P}66)-MMP

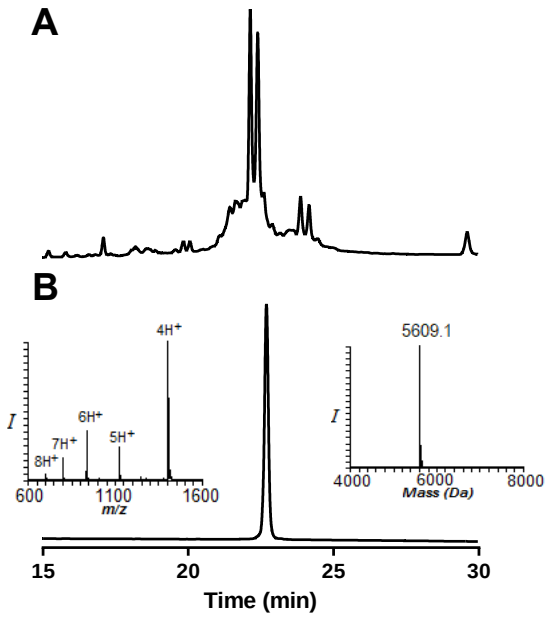

Figure S4. (A) HPLC of crude Thz-p19^{INK4d}(56-107)(S^{P}66)-MeDbz. (B) HPLC and mass analysis of purified fragment **7**, Thz-p19^{INK4d}(56-107)(S^{P}66)-MMP with observed mass of 5609.1 ± 0.2 Da (calculated 5609.0 Da).

6. Synthesis of Thz-p19^{INK4d}(56-107)(S^{P}76)-MMP

Synthesis, analysis, and purification were carried out in the same manner as described for fragment **2** (Scheme S2) to obtain the fragment **8**, Thz-p19^{INK4d}(56-107)(S^{P}76)-MMP in 21.2 % isolated yield (238 mg from 0.2 mmol).

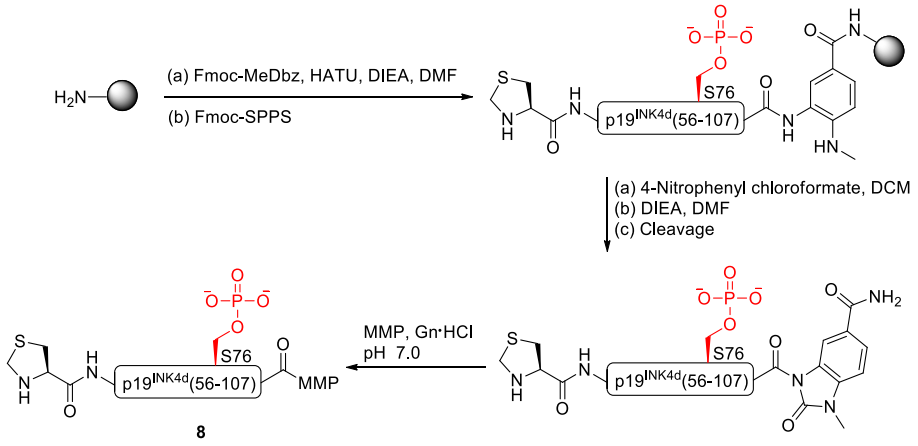

Scheme S5. Synthetic steps for Thz-p19^{INK4d}(56-107)(S^{P}76)-MMP.

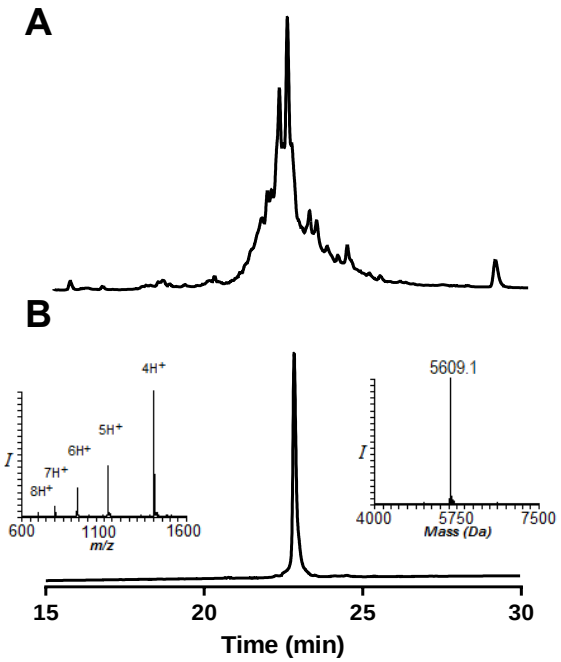

Figure S5. (A) HPLC of crude Thz-p19^{INK4d}(56-107)(S^{P}76)-MeDbz. (B) HPLC and mass analysis of purified fragment **8**, Thz-p19^{INK4d}(56-107)(S^{P}76)-MMP with observed mass of 5609.1 ± 0.2 Da (calculated 5609.0 Da).

7. Synthesis of fragment 4, p19^{INK4d}(2-54)-MMP

The synthesis was carried out on Knorr Resin (0.26 mmol/g, 0.2 mmol scale). Fmoc-Dbz (4 equiv) was coupled to the resin using HBTU (4 equiv), HOBT (4 equiv) and DIEA (8 equiv) for 90 min. Pseudoproline dipeptides, Fmoc-Ser(tBu)-Thr(psiMe,Mepro)-OH, Fmoc-Lys(Boc)-Thr(psiMe,Mepro)-OH, and Fmoc-Leu-Ser(ψMe,Mepro)-OH respectively were coupled manually using 2.5 equiv of the dipeptide and 2.5 equiv HATU and 5 equiv of DIEA for 90 min at positions Ser53-Thr54, Lys43-Thr44 and Leu12-Ser13, respectively. The other amino acids were coupled using standard Fmoc-SPPS on peptide synthesizer. After completion of SPPS, the peptide on the resin (0.1 mmol) was treated with p-nitrophenyl chloroformate (100 mg, 5 equiv) in 4 ml dry DCM for 30 min (3 cycles) and washed with DCM and DMF followed by treatment in 4 ml of 0.5 M DIEA in DMF for 10 min (3 cycles). Peptide cleavage was carried using the cocktail of TFA: triisopropylsilane: water (95: 2.5: 2.5). The crude peptide (25 mg) was dissolved in 6 M Gn·HCl/200 mM phosphate buffer (pH 7.0, 1.5 ml) containing MMP (200 equiv, 56 μl), and incubated at 37 ºC for 1 h. The progress of the reaction was monitored, and the product was purified using HPLC with a gradient of 0-60% B in 30 min to obtain fragment **4**, p19(2-54)-MMP in 16.5 % isolated yield (197 mg from 0.2 mmol).

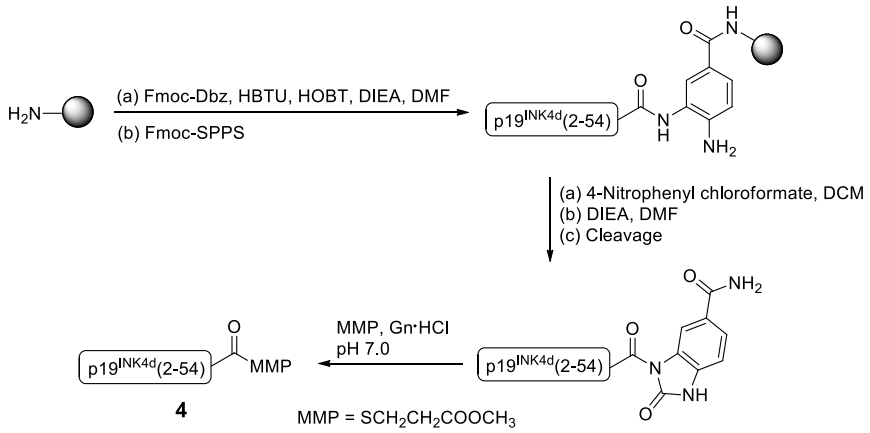

Scheme S6. Synthetic steps for p19^{INK4d}(2-54)-MMP.

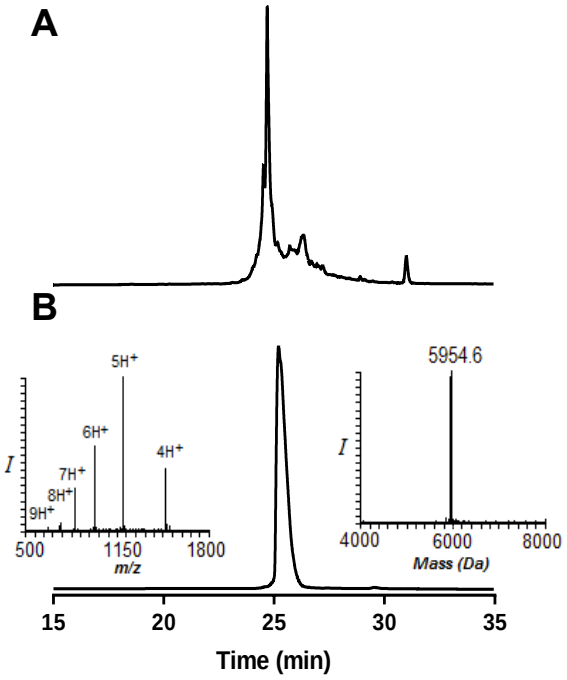

Figure S6. (A) HPLC of crude p19^{INK4d}(2-54)-Dbz. (B) HPLC and mass analysis of purified fragment **4**, p19^{INK4d}(2-54)-MMP with observed mass of 5954.6 ± 0.2 Da (calculated 5954.7 Da).

8. Synthesis of HA-p19^{INK4d}(2-54)-MMP

Synthesis, analysis, and purification were carried out in the same manner as described for fragment **4** (Scheme S6) to obtain the fragment **9**, HA-p19^{INK4d}(2-54)-MMP in 15.4 % isolated yield (217 mg from 0.2 mmol).

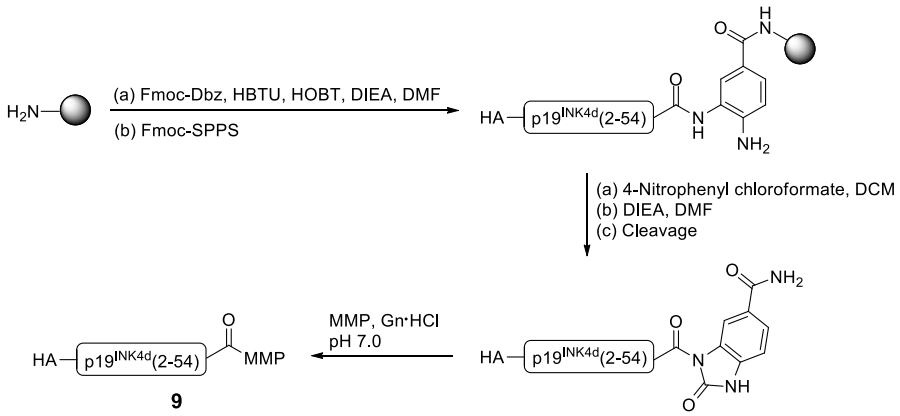

Scheme S7. Synthetic steps for HA-p19^{INK4d}(2-54)-MMP.

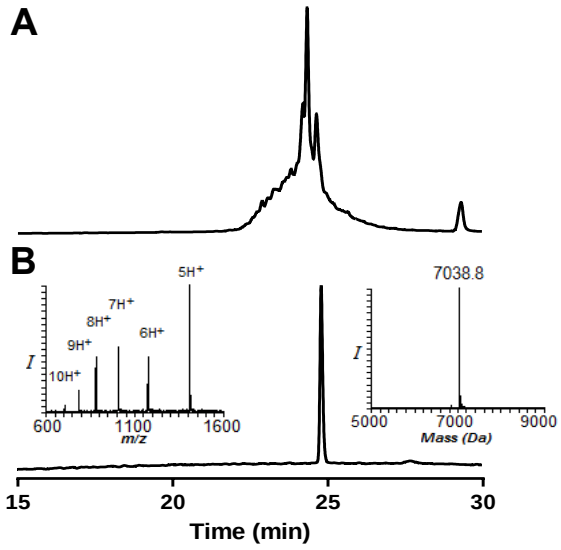

Figure S7. (A) HPLC of crude HA-p19^{INK4d}(2-54)-Dbz. (B) HPLC and mass analysis of purified fragment **9**, HA-p19^{INK4d}(2-54)-MMP with observed mass of 7038.8 ± 0.3 Da (calculated 7038.8 Da).

9. Synthesis of peptide 3, Cys-p19^{INK4d}(56-166)(S^{P}66 & S^{P}76)

Cys-p19(107-165), fragment **1**, (12.7 mg, 2.0×10^{-3} mmol) and Thz-p19(56-106)(S^{P}66 & S^{P}76)-MMP, fragment **2**, (14.8 mg, 2.6×10^{-3} mmol) were dissolved in 6 M Gn·HCl/200 mM phosphate buffer (pH 7.0, 660 µL) containing MPAA (60 mM) and TCEP (30 mM). After incubation at 37 ºC for 1 h, $MgCl_2$ (100 equiv, 19 mg) was added to the reaction mixture, which was further incubated for 10 min at 37ºC. Then the reaction mixture was treated with $[Pd(allyl)Cl]_2$ (15 equiv, 11.0 mg) and incubated at 37 ºC for 1 h to unmask the Thz. The reaction was quenched by adding 60 equiv of DTT, followed by centrifugation to pellet the solid material and the supernatant was further analyzed. The progress of the reaction was monitored and the product was purified using HPLC with a gradient of 25-65% B in 40 min to obtain peptide **3**, Cys-p19^{INK4d}(56-166)(S^{P}66 & S^{P}76) (10 mg, 42 % yield).

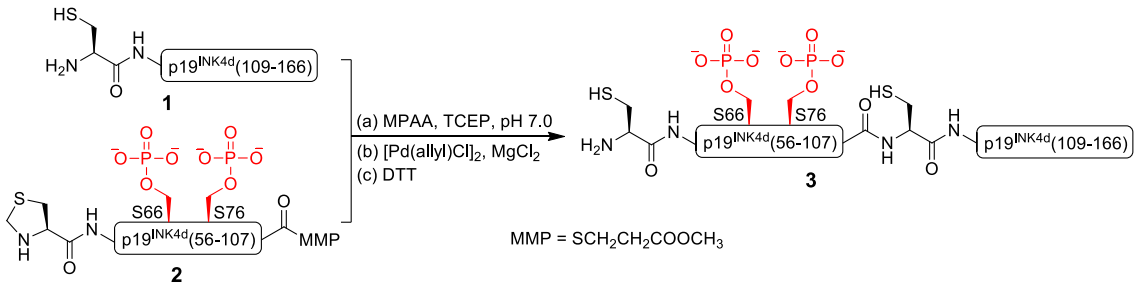

Scheme S8. Synthetic steps for peptide **3**, Cys-p19^{INK4d}(56-166)(S^{P}66 & S^{P}76).

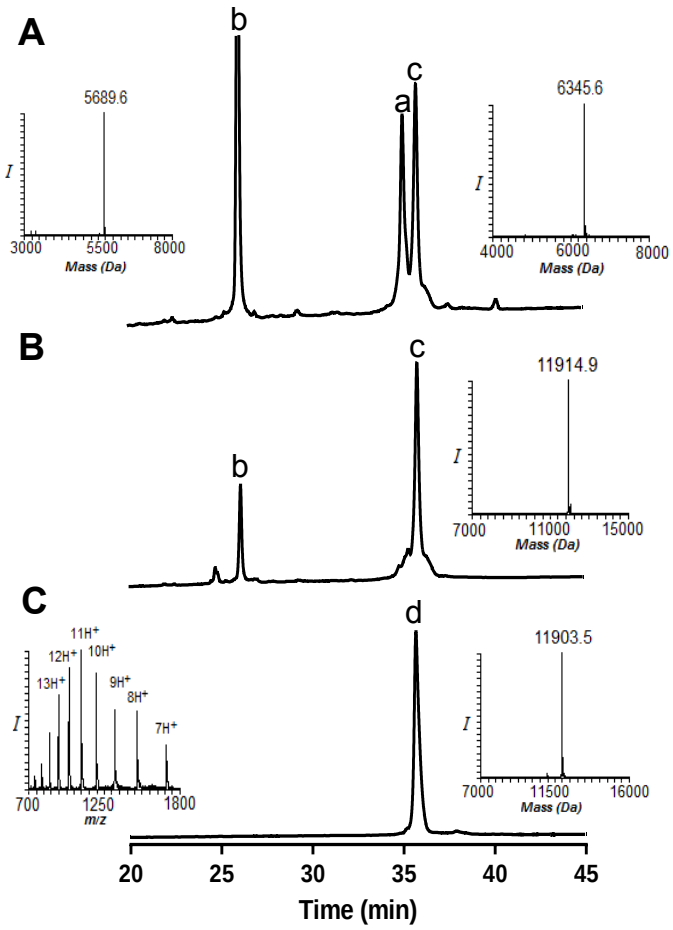

Figure S8. (A) HPLC and mass traces of the ligation mixture at time 0: Peak a corresponds to Cys-p19^{INK4d}(109-166), fragment **1** (6345.6 Da), and peak b corresponds to Thz-p19^{INK4d}(56-106)(S^{P}66 & S^{P}76)-MMP, fragment **2** (5689.6 Da). (B) HPLC of the ligation mixture after 1 h: Peak c corresponds to the ligation product with observed mass of 11914.9 ± 0.8 Da (calculated 11913.3 Da). (C) HPLC of purified Cys-p19^{INK4d}(56-166)(S^{P}66 & S^{P}76), peptide **3**: Peak d with observed mass of 11903.5 ± 0.8 Da (calculated 11901.4 Da).

10. Synthesis of Cys-p19^{INK4d}(56-166)

Synthesis, analysis, and purification were carried out in the same manner as described for peptide **3** (Scheme S8) to obtain peptide **10**, Cys-p19^{INK4d}(56-166) in 44 % isolated yield.

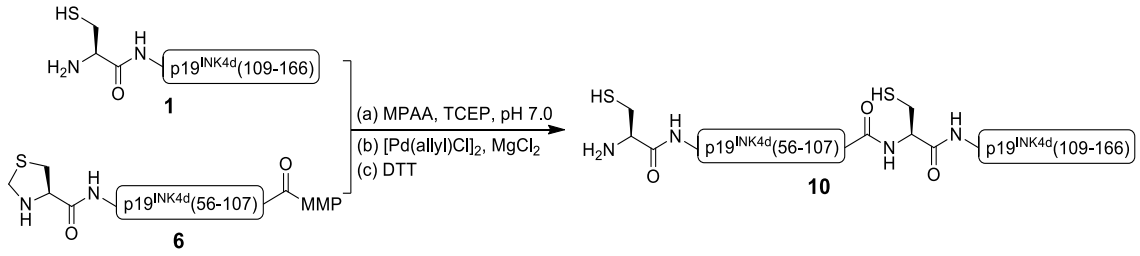

Scheme S9. Synthetic steps for Cys-p19^{INK4d}(56-166).

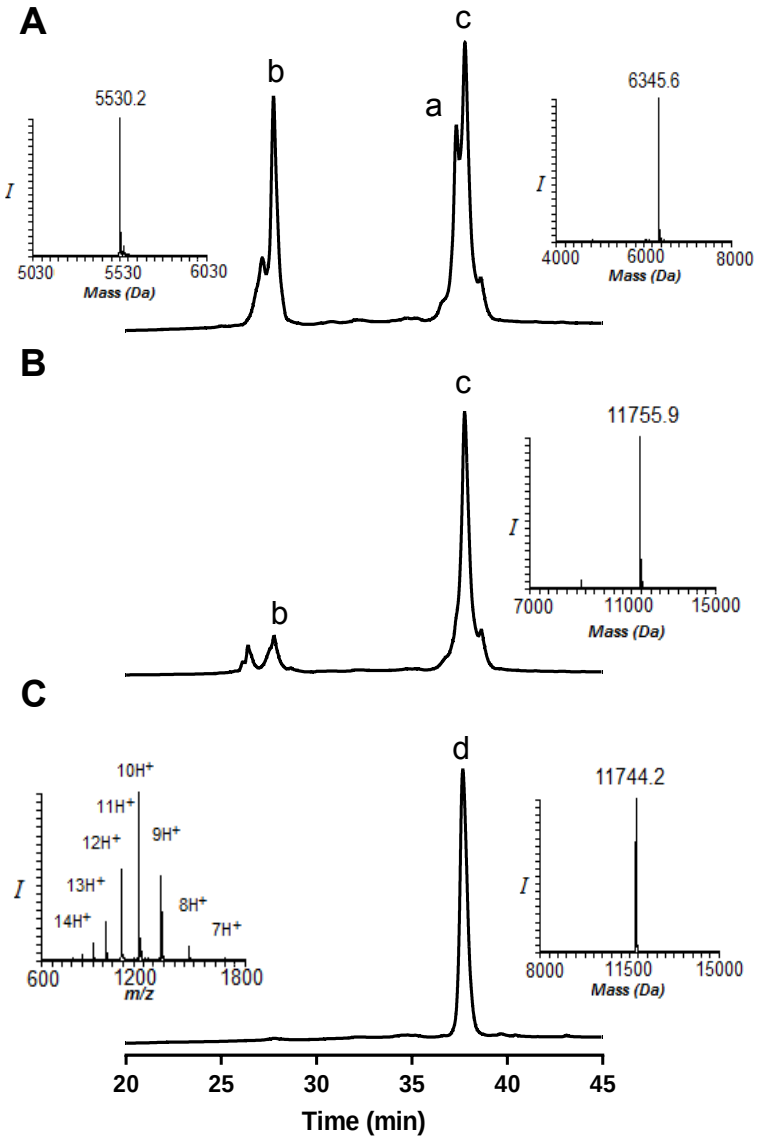

Figure S9. (A) HPLC and mass traces of the ligation mixture at time 0: Peak a corresponds to Cys-p19^{INK4d}(109-166), fragment **1** (6345.6 Da), and peak b corresponds to Thz-p19^{INK4d}(56-106)-MMP, fragment **6** (5530.2 Da). (B) HPLC of the ligation mixture after 1 h: Peak c corresponds to the ligation product with observed mass of 11755.9 ± 0.8 Da (calculated 11755.4 Da). (C) HPLC of purified Cys-p19^{INK4d}(56-166), peptide **10**: Peak d with observed mass of 11744.2 ± 0.8 Da (calculated 11743.4 Da).

11. Synthesis of Cys-p19^{INK4d}(56-166)(S^{P}66)

Synthesis, analysis, and purification were carried out in the same manner as described for peptide **3** (Scheme S8) to obtain peptide **11**, Cys-p19^{INK4d}(56-166)(S^{P}66) in 43 % isolated yield.

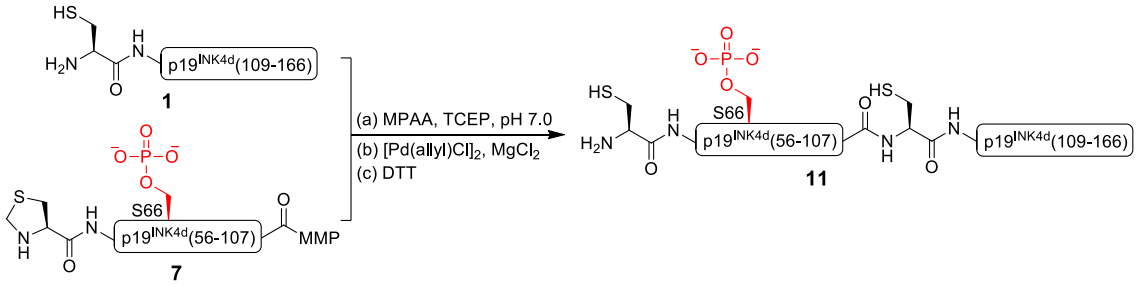

Scheme S10. Synthetic steps for Cys-p19^{INK4d}(56-166)(S^{P}66).

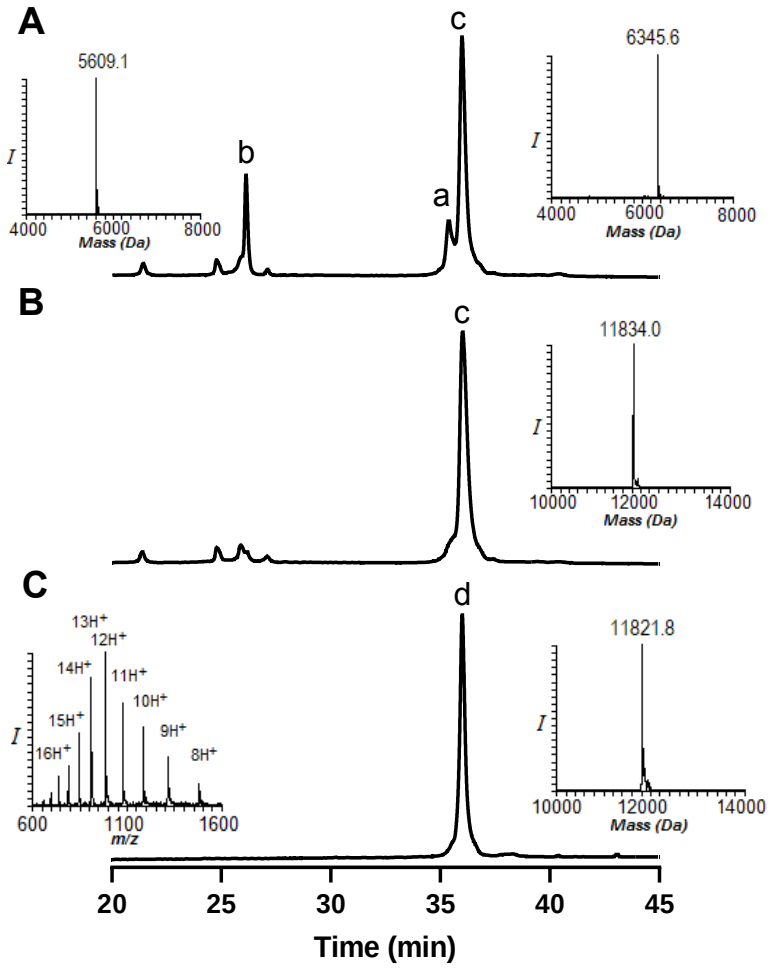

Figure S10. (A) HPLC and mass traces of the ligation mixture at time 0: Peak a corresponds to Cys-p19^{INK4d}(109-166), fragment **1** (6345.6 Da), and peak b corresponds to Thz-p19^{INK4d}(56-106)(S^{P}66)-MMP, fragment **7** (5609.1 Da). (B) HPLC of the ligation mixture after 1 h: Peak c corresponds to the ligation product with observed mass of 11834.0 ± 0.8 Da (calculated 11834.4 Da). (C) HPLC of purified Cys-p19^{INK4d}(56-166)(S^{P}66): Peak d corresponds to peptide **11** with observed mass of 11821.8 ± 0.8 Da (calculated 11822.4 Da).

12. Synthesis of Cys-p19^{INK4d}(56-166)(S^{P}76)

Synthesis, analysis, and purification were carried out in the same manner as described for peptide **3** (Scheme S8) to obtain the peptide **12**, Cys-p19^{INK4d}(56-166)(S^{P}76) in 43 % isolated yield.

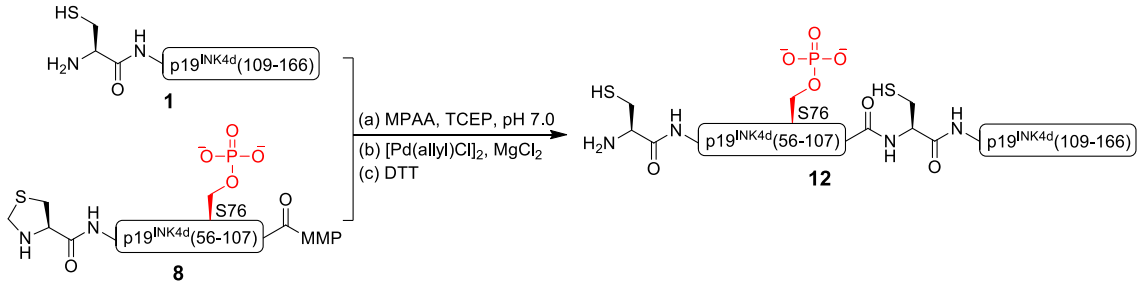

Scheme S11. Synthetic steps for Cys-p19^{INK4d}(56-166)(S^{P}76).

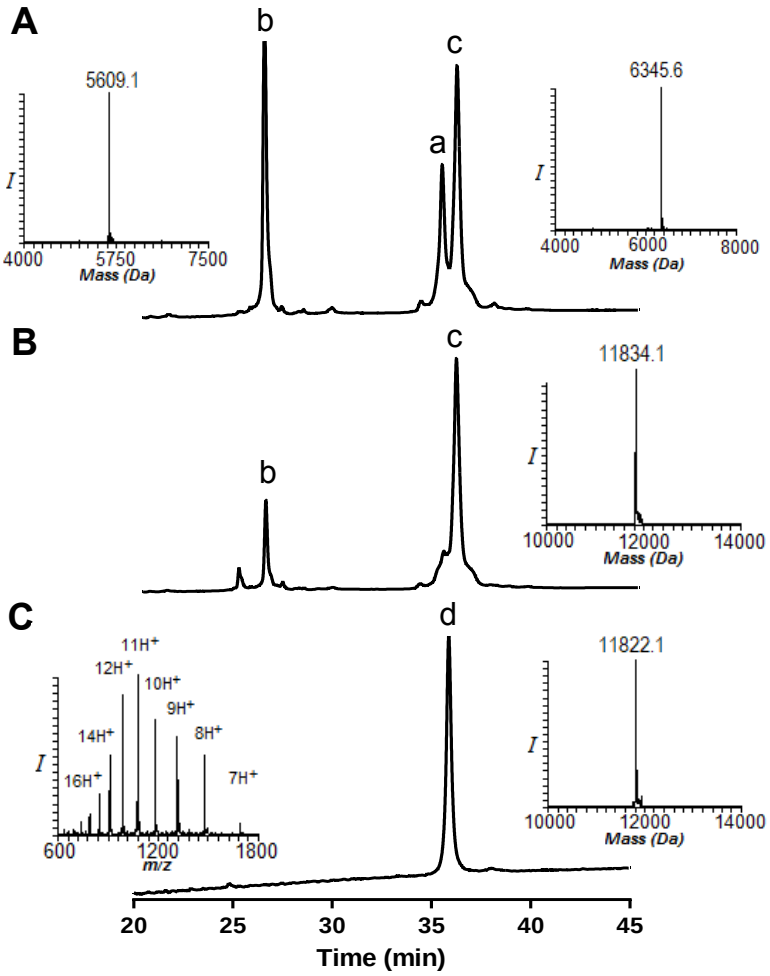

Figure S11. (A) HPLC and mass traces of the ligation mixture at time 0: Peak a corresponds to Cys-p19^{INK4d}(109-166), fragment **1** (6345.6 Da), and peak b corresponds to Thz-p19^{INK4d}(56-106)(S^{P}76)-MMP, fragment **8** (5609.1 Da). (B) HPLC of the ligation mixture after 1 h: Peak c corresponds to the ligation product with observed mass of 11834.1 ± 0.8 Da (calculated 11834.4 Da). (C) HPLC of purified Cys-p19^{INK4d}(56-166)(S^{P}76): Peak d corresponds to peptide **12** with observed mass of 11822.1 ± 0.8 Da (calculated 11822.4 Da).

13. Synthesis of 5, p19^{INK4d}(2-166)(S^{P}66 & S^{P}76)

Cys-p19^{INK4d}(56-166)(S^{P}66 & S^{P}76), peptide **3**, (6.0 mg, 5.0×10^{-4} mmol) and p19^{INK4d}(2-54)-MMP, fragment **4**, (7.4 mg, 1.25×10^{-3} mmol) were dissolved in 6 M Gn·HCl, 200 mM phosphate buffer (pH 7.2, 330 μL) containing MPAA (150 mM) and TCEP (75 mM). The reaction was incubated at 37 ºC and completed in 20 h. Then the collected crude ligation product was subjected to radical desulfurization by dissolving it in 6 M Gn·HCl/200 mM phosphate buffer (1.5 mM) and treatment with TCEP (250 mM), VA-044 (80 equiv) and tert-butyl thiol (10% of reaction volume) at 37 °C for 5-6 h. The progress of the reaction was monitored and the product was purified using HPLC with a gradient of 25-65% B in 40 min to obtain **5**, p19^{INK4d}(2-166)(S^{P}66 & S^{P}76) in ~18 % isolated yield (1.6 mg).

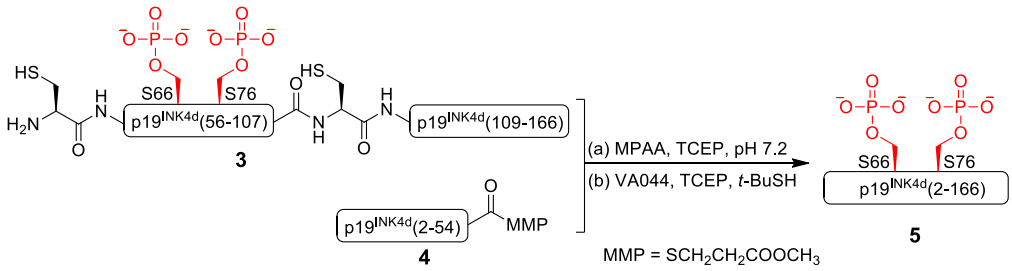

Scheme S12. Synthetic steps for **5**, p19^{INK4d}(2-166)(S^{P}66 & S^{P}76).

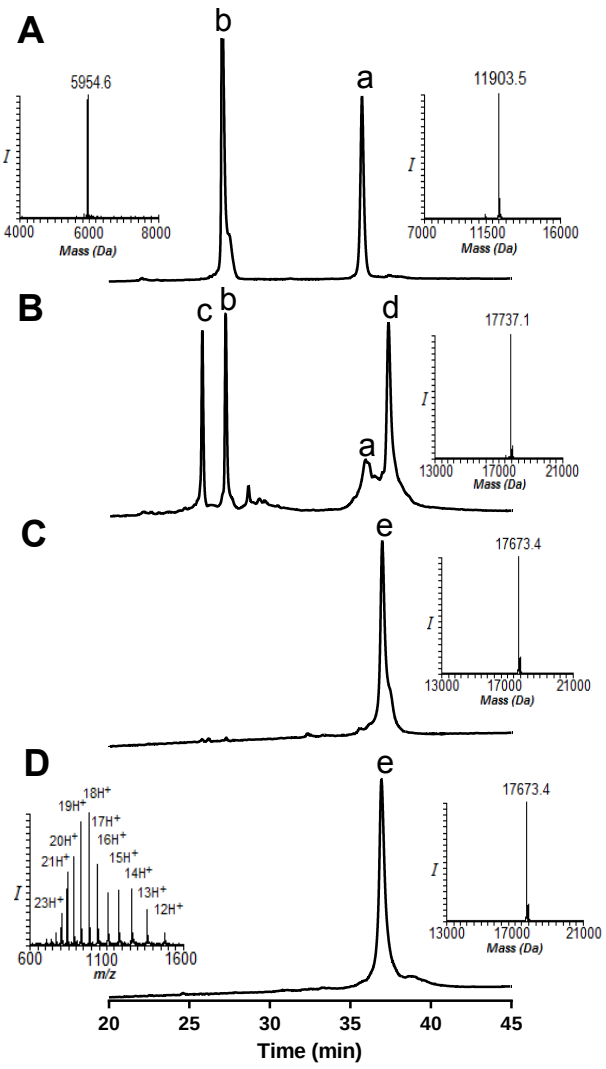

Figure S12. (A) HPLC and mass traces of the ligation mixture at time 0: Peak a corresponds to Cys-p19^{INK4d}(56-166)(S^{P}66 & S^{P}76), peptide **3** (11903.5 Da), and peak b corresponds to p19^{INK4d}(2-54)-MMP, fragment **4** (5954.6 Da). (B) HPLC of the ligation mixture after 20 h: Peak c corresponds to the fragment **4** hydrolysis product p19^{INK4d}(2-54)-COOH, and peak d corresponds to the ligation product with observed mass of 17737.1 ± 1.6 Da (calculated 17736.0 Da). (C) HPLC of the desulfurization after 4 h: Peak e corresponds to the desulfurization product with observed mass of 17673.4 ± 2.1 Da (calculated 17671.9 Da). (D) HPLC of purified **5**, p19^{INK4d}(2-166)(S^{P}66 & S^{P}76).

14. Synthesis of p19^{INK4d}(2-166)(WT)

Synthesis, analysis, and purification were carried out in the same manner as described for protein **5** (Scheme S12) to obtain **13**, p19^{INK4d}(2-166)(WT) in ~18 % isolated yield.

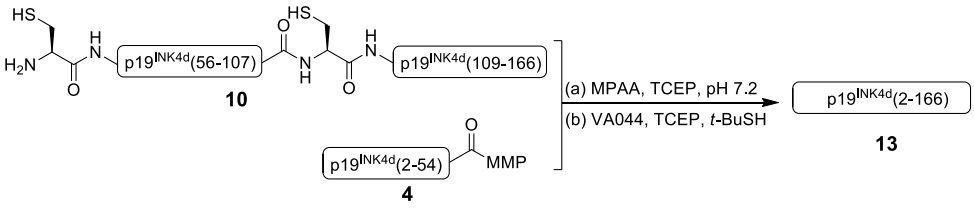

Scheme S13. Synthetic steps for p19^{INK4d}(2-166)(WT).

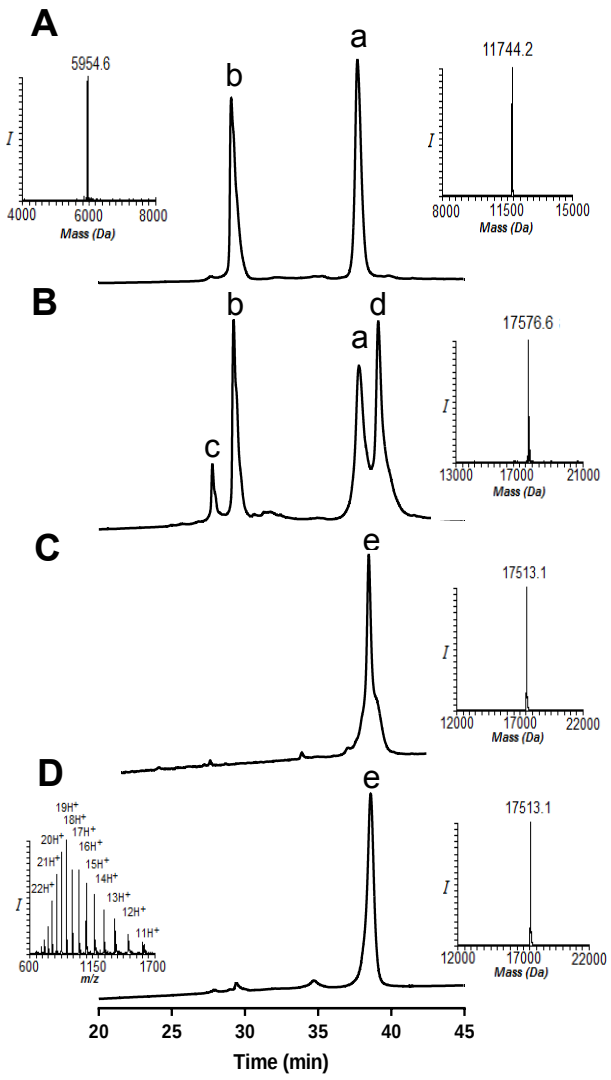

Figure S13. (A) HPLC and mass traces of the ligation mixture at time 0: Peak a corresponds to Cys-p19^{INK4d}(56-166), peptide **10** (11744.2 Da), and peak b corresponds to p19^{INK4d}(2-54)-MMP, fragment **4** (5954.6 Da). (B) HPLC of the ligation mixture after 8 h: Peak c corresponds to the fragment **4** hydrolysis product p19^{INK4d}(2-54)-COOH, and peak d corresponds to the ligation product with observed mass of 17576.6 ± 1.6 Da (calculated 17578.0 Da). (C) HPLC of desulfurization reaction after 4 h: Peak e corresponds to the desulfurized product with observed mass of 17513.1 ± 2.1 Da (calculated 17513.9 Da). (D) HPLC of purified **13**, p19^{INK4d}(2-166)(WT).

15. Synthesis of p19^{INK4d}(2-166)(S^{P}66)

Synthesis, analysis, and purification were carried out in the same manner as described for protein **5** (Scheme S12) to obtain **14**, p19^{INK4d}(2-166)(S^{P}66) in ~18 % isolated yield.

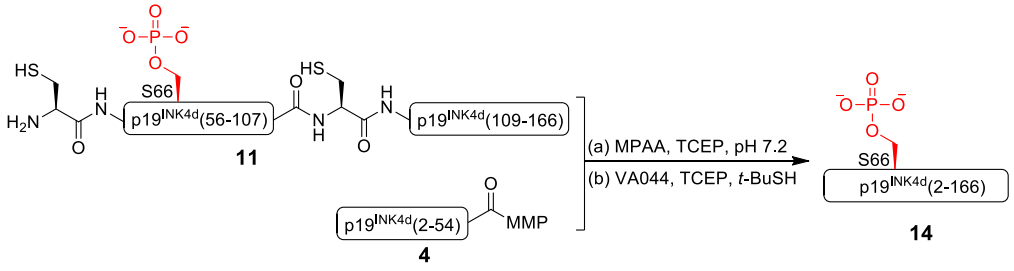

Scheme S14. Synthetic steps for p19^{INK4d}(2-166)(S^{P}66).

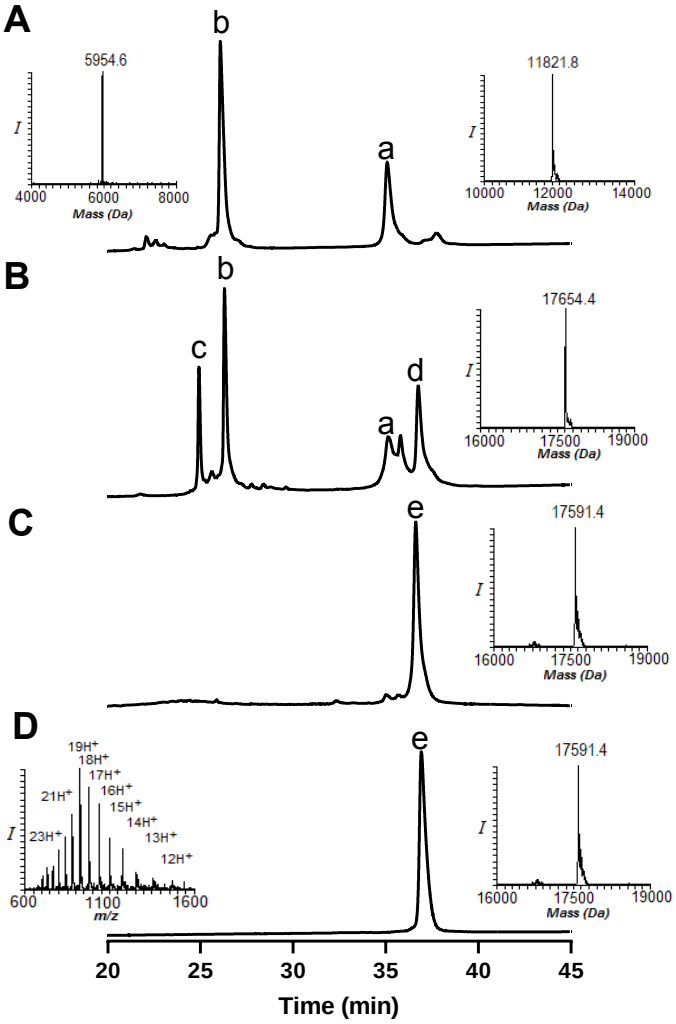

Figure S14. (A) HPLC and mass traces of the ligation mixture at time 0: Peak a corresponds to Cys-p19^{INK4d}(56-166)(S^{P}66), peptide **11** (11821.8 Da), and peak b corresponds to p19^{INK4d}(2-54)-MMP, fragment **4** (5954.6 Da). (B) HPLC of the ligation mixture after 12 h: Peak c corresponds to hydrolysis product p19^{INK4d}(2-54)-COOH, and peak d corresponds to the ligation product with observed mass of 17654.4 ± 1.6 Da (calculated 17657.0 Da). (C) HPLC of the desulfurization reaction after 4 h: Peak e corresponds to the desulfurized product with observed mass of 17591.4 ± 2.1 Da (calculated 17592.9 Da). (D) HPLC of purified **14**, p19^{INK4d}(2-166)(S^{P}66).

16. Synthesis of p19^{INK4d}(2-166)(S^{P}76)

Synthesis, analysis, and purification were carried out in the same manner as described for protein **5** (Scheme S12) to obtain **15**, p19^{INK4d}(2-166)(S^{P}76) in ~18 % isolated yield.

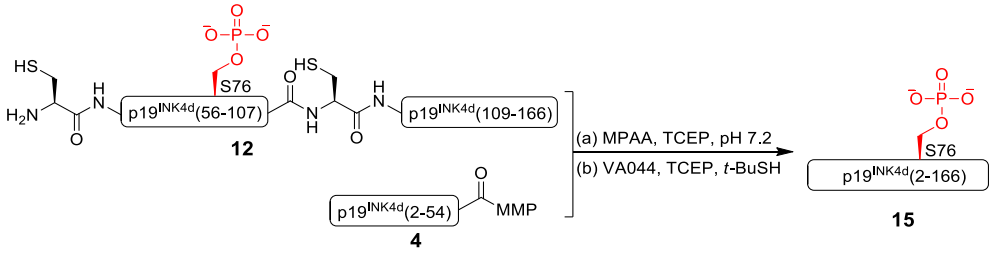

Scheme S15. Synthetic steps for p19^{INK4d}(2-166)(S^{P}76).

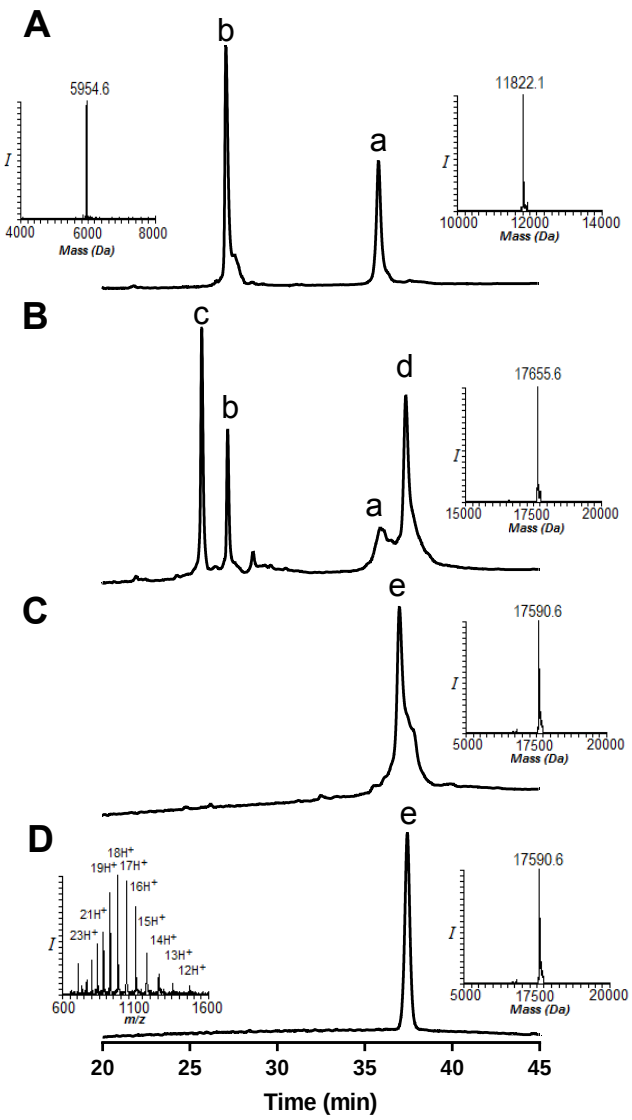

Figure S15. (A) HPLC and mass traces of the ligation mixture at time 0: Peak a corresponds to Cys-p19^{INK4d}(56-166)(S^{P}66), peptide **12** (11822.1 Da), and peak b corresponds to p19^{INK4d}(2-54)-MMP, fragment **4** (5954.6 Da). (B) HPLC of the ligation mixture after 20 h: Peak c corresponds to the hydrolysis product p19^{INK4d}(2-54)-COOH, and peak d corresponds to the ligation product with observed mass of 17655.6 ± 1.6 Da (calculated 17657.0 Da). (C) HPLC of the desulfurization after 4 h: Peak e corresponds to the desulfurized product with observed mass of 17590.6 ± 2.1 Da (calculated 17592.9 Da). (D) HPLC of purified **15**, p19^{INK4d}(2-166)(S^{P}76).

17. Synthesis of HA-p19^{INK4d}(2-166)(S^{P}66 & S^{P}76)

Synthesis, analysis, and purification were carried out in the same manner as described for protein **5** (Scheme S12) to obtain **16**, HA-p19^{INK4d}(2-166)(S^{P}66 & S^{P}76) in ~18 % isolated yield.

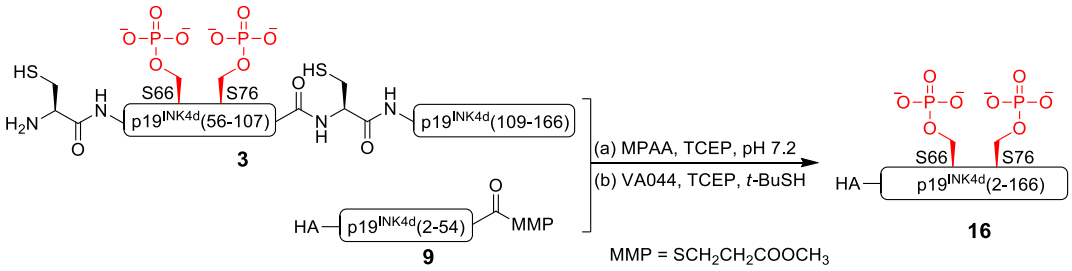

Scheme S16. Synthetic steps for HA-p19^{INK4d}(2-166)(S^{P}66 & S^{P}76).

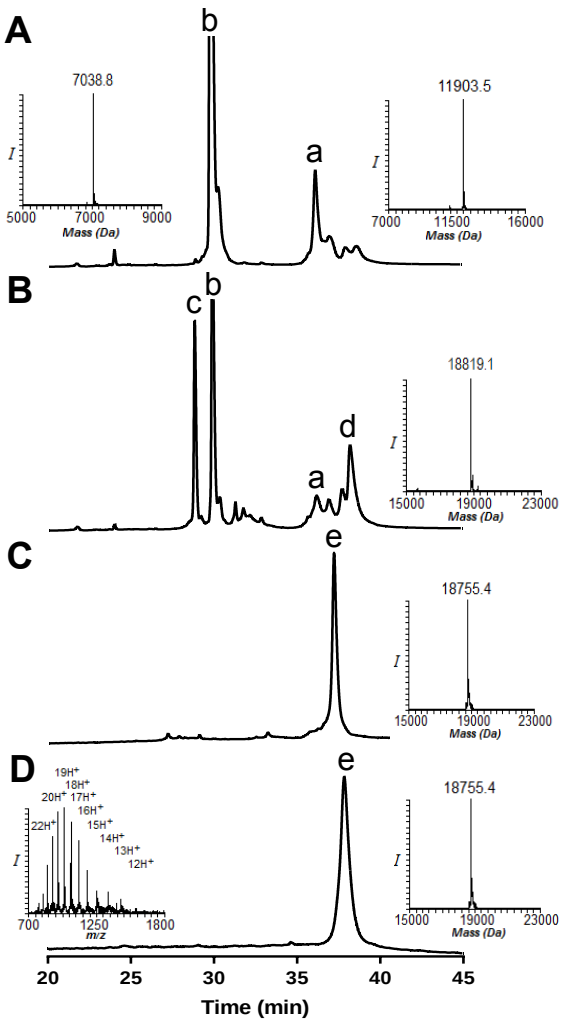

Figure S16. (A) HPLC and mass traces of the ligation mixture at time 0: Peak a corresponds to Cys-p19^{INK4d}(56-166)(S^{P}66 & S^{P}76), peptide **3** (11903.5 Da), and peak b corresponds to HA-p19^{INK4d}(2-54)-MMP, fragment **9** (7038.8 Da). (B) HPLC of the ligation mixture after 10 h: Peak c corresponds to the fragment **9** hydrolysis product HA-p19^{INK4d}(2-54)-COOH, and peak d corresponds to the ligation product with observed mass of 18819.1 ± 1.8 Da (calculated 18820.2 Da). (C) HPLC of the desulfurization after 4 h: Peak e corresponds to the desulfurized product with observed mass of 18755.4 ± 2.3 Da (calculated 18756.1 Da). (D) HPLC of purified **16**, HA-p19^{INK4d}(2-166)(S^{P}66 & S^{P}76).

18. Synthesis of HA-p19^{INK4d}(2-166)(WT)

Synthesis, analysis, and purification were carried out in the same manner as described for protein **5** (Scheme S12) to obtain **17**, HA-p19^{INK4d}(2-166)(WT) in ~18 % isolated yield.

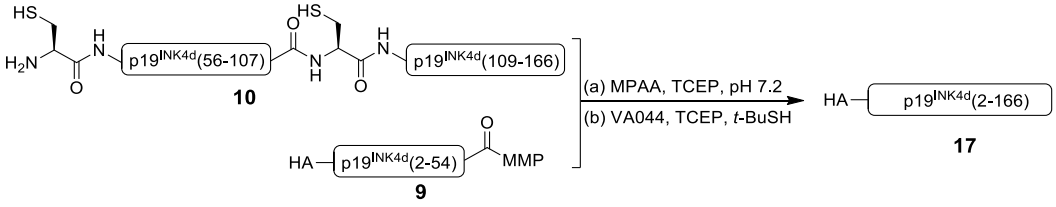

Scheme S17. Synthetic steps for HA-p19^{INK4d}(2-166)(WT).

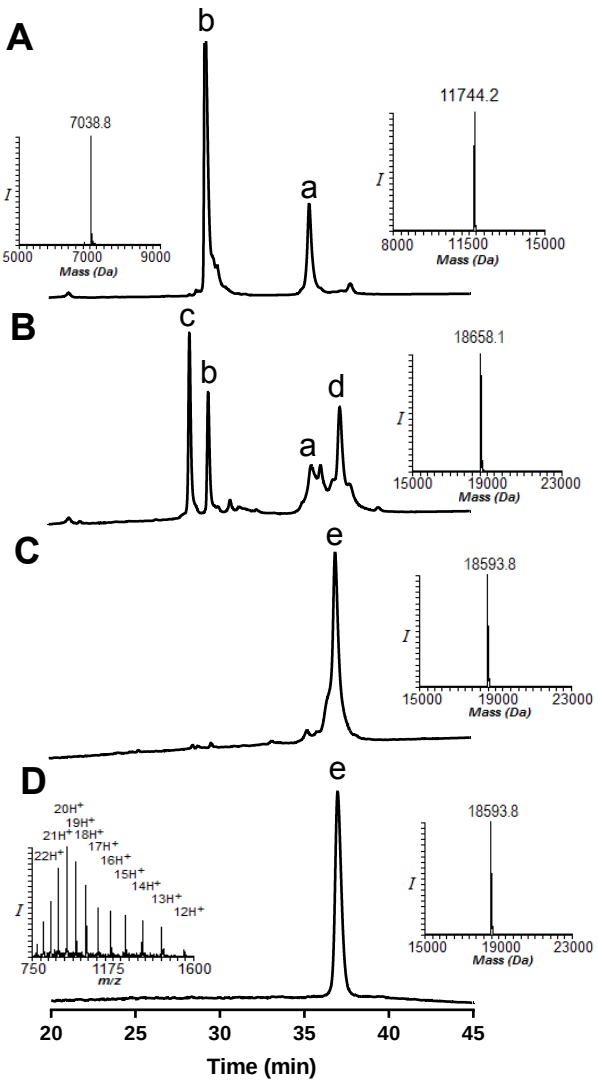

Figure S17. (A) HPLC and mass traces of the ligation mixture at time 0: Peak a corresponds to Cys-p19^{INK4d}(56-166), peptide **10** (11744.2 Da), and peak b corresponds to HA-p19^{INK4d}(2-54)-MMP, fragment **9** (7038.8 Da). (B) HPLC of the ligation mixture after 10 h: Peak c corresponds to the fragment **9** hydrolysis product HA-p19^{INK4d}(2-54)-COOH, and peak d corresponds to the ligation product with observed mass of 18658.1 ± 1.8 Da (calculated 18662.2 Da). (C) HPLC of the desulfurization after 4 h: Peak e corresponds to the desulfurized product with observed mass of 18593.8 ± 2.3 Da (calculated 18598.1 Da). (D) HPLC of purified **17**, HA-p19^{INK4d}(2-166) WT.

19. Synthesis of HA-p19^{INK4d}(2-166)(S^{P}66)

Synthesis, analysis, and purification were carried out in the same manner as described for protein **5** (Scheme S12) to obtain **18**, HA-p19^{INK4d}(2-166)(S^{P}66) in ~18 % isolated yield.

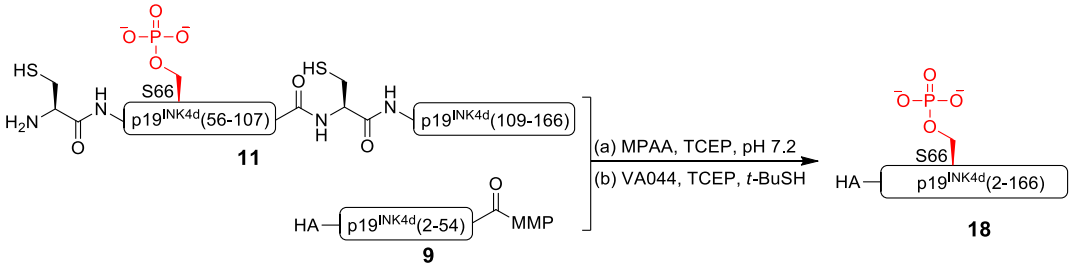

Scheme S18. Synthetic steps for HA-p19^{INK4d}(2-166)(S^{P}66).

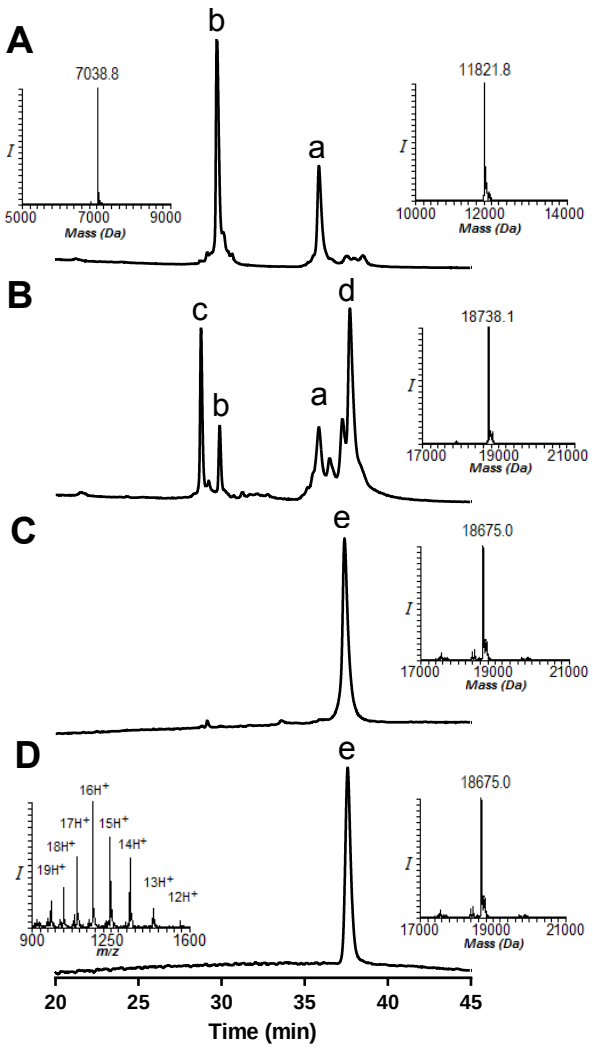

Figure S18. (A) HPLC and mass traces of the ligation mixture at time 0: Peak a corresponds to Cys-p19^{INK4d}(56-166)(S^{P}66), peptide **11** (11821.8 Da), and peak b corresponds to HA-p19^{INK4d}(2-54)-MMP, fragment **9** (7038.8 Da). (B) HPLC of the ligation mixture after 15 h: Peak c corresponds to the fragment **9** hydrolysis product HA-p19^{INK4d}(2-54)-COOH, and peak d corresponds to the ligation product with observed mass of 18738.1 ± 1.8 Da (calculated 18741.2 Da). (C) HPLC of the desulfurization after 4 h: Peak e corresponds to the desulfurized product with observed mass of 18675.0 ± 2.3 Da (calculated 18677.1 Da). (D) HPLC of purified **18**, HA-p19^{INK4d}(2-166)(S^{P}66).

20. Synthesis of HA-p19^{INK4d}(2-166)(S^{P}76)

Synthesis, analysis, and purification were carried out in the same manner as described for protein **5** (Scheme S12) to obtain **19**, HA-p19^{INK4d}(2-166)(S^{P}76) in ~18 % isolated yield.

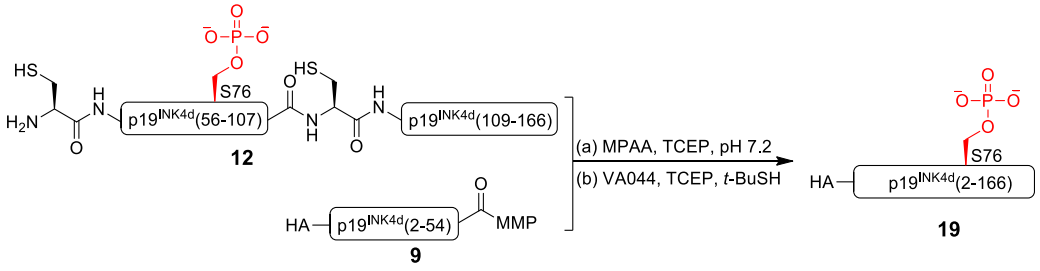

Scheme S19. Synthetic steps for HA-p19^{INK4d}(2-166)(S^{P}76).

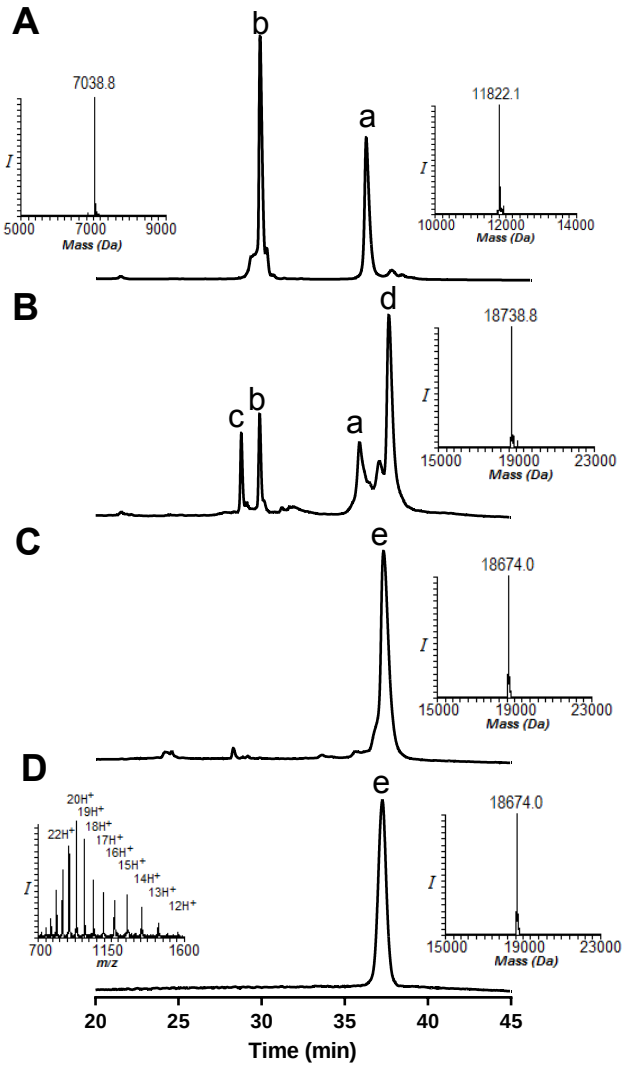

Figure S19. (A) HPLC and mass traces of the ligation mixture at time 0: Peak a corresponds to Cys-p19^{INK4d}(56-166)(S^{P}66), peptide **12** (11822.1 Da), and peak b corresponds to HA-p19^{INK4d}(2-54)-MMP, fragment **9** (7038.8 Da). (B) HPLC of the ligation mixture after 15 h: Peak c corresponds to the fragment **9** hydrolysis product HA-p19^{INK4d}(2-54)-COOH, and peak d corresponds to the ligation product with observed mass of 18738.8 ± 1.8 Da (calculated 18741.2 Da). (C) HPLC of the desulfurization after 4 h: Peak e corresponds to the desulfurized product with observed mass of 18674.0 ± 2.3 Da (calculated 18677.1 Da). (D) HPLC of purified **19**, HA-p19^{INK4d}(2-166)(S^{P}76).

21. P19^{INK4d} folding

Aqueous buffers such as tris, sodium phosphate and sodium acetate at both high and low pH (pH 7.4 and pH 4.0), with and without 150 mM of NaCl failed to properly fold the p19^{INK4d} analogues and resulted in their precipitation and aggregation leading to low concentration and low CD (Circular Dichroism) signal. We overcame this by adding 25% glycerol which stabilized the protein folding in solution. Stock solutions were made by dissolving a small amount of each analogue (0.2-0.5 mg) in 6 M Gn·HCl (10-20 μl). From the stock solution, 3 or 5 μL of protein in Gn·HCl were taken and rapidly folded by adding 50 mM sodium phosphate in 25 % glycerol to a final volume of 150 μL or 250 μL respectively (2% 6 M Gn·HCl). The folded solutions were spun down, and the clear solutions were collected, left on ice for 1 h and the samples were kept in -80 ºC after freezing in liquid nitrogen.

22. CD measurements

Samples were thawed and kept on ice throughout the whole process. Concentrations for the 4 analogues were determined using Bradford assay concurrently before measuring CD for all the samples on the same day. CD measurements were performed using a circular dichroism spectrometer Model Jasco 810 Spectropolarimeter and AppliedPhotophysics Chirascan. The ellipticity was measured as a function of wavelength at different temperatures for the wavelength range of 200-270 nm at 10 ºC, 25 ºC, and 37 ºC using 0.1 cm cuvette (200 μL volume) with a scan time of 1 sec per wavelength. The concentration used ranged between 4 μM and 10 μM.

Since glycerol and Gn·HCl were required in the folding causing a high voltage (HV) at the far-UV wavelengths during measurement, the interpretation of the curve changes in increasing temperature between 200-204 nm is irrelevant. Thermal-denaturation scans measurements were performed between 10-70 ºC for all the 4 analogues consecutively, in 0.05 cm cuvette (100 µl volume) at 222 nm and 208 nm wavelength, with a scan time of 2.5 sec per wavelength. Scans were taken in an interval of 0.2 ºC with a heating rate of 1 ºC/min, at which each thermal curve was completed in 60 min. Concentrations used for thermal scans were between 7 µM to 16 µM to acquire a high signal to noise ratio at higher temperatures. It is worth mentioning that the thermal unfolding of $p19^{INK4d}$ analogues at the conditions we tested is irreversible. Therefore, thermodynamic characterization of the analogues was not carried out.

Calculations

The folded fraction in increasing temperature was calculated at both 222 nm and 208 nm wavelengths using equation 1 where θ_t is the observed ellipticity at any temperature, θ_U is the ellipticity for the unfolded form of the protein and θ_F is the ellipticity of the folded protein (the measured ellipticity is subtracted from the buffer contribution to obtain the actual ellipticity of the samples at each measured point). The melting point (Tm) is where α=0.5 at which half of the proteins are in their unfolded state.

1. $\alpha = \frac{\theta_t - \theta_U}{\theta_F - \theta_U}$

Since the thermal-denaturation curve can be fitted into a sigmoidal curve, equation 2 known as Boltzmann sigmoid equation was used to calculate the Tm of each curve, where Y is the folded fraction and X is the measured temperature. Different ranges of temperature

were taken to calculate the Tm, according to the position of the transition. Thus, for $p19^{INK4d}$(WT) and $p19^{INK4d}(S^P66)$ -the more stable analogues, values from 30 ºC to 70 ºC were used, while for $p19^{INK4d}(S^P76)$ and $p19^{INK4d}(S^P66$ & $S^P76)$ values from 10 ºC to 55 ºC were used to calculate the Tm .

2. $Y = \frac{1}{1+\exp(\frac{Tm-X}{slope})}$

Using non-linear regression analysis, the Tm was extrapolated. Only the data which gave a Boltzmann fit accuracy of $R^2 \geq 0.97$ at both 222 nm and 208 nm curves for the measured sample were presented and used to calculate the average Tm.

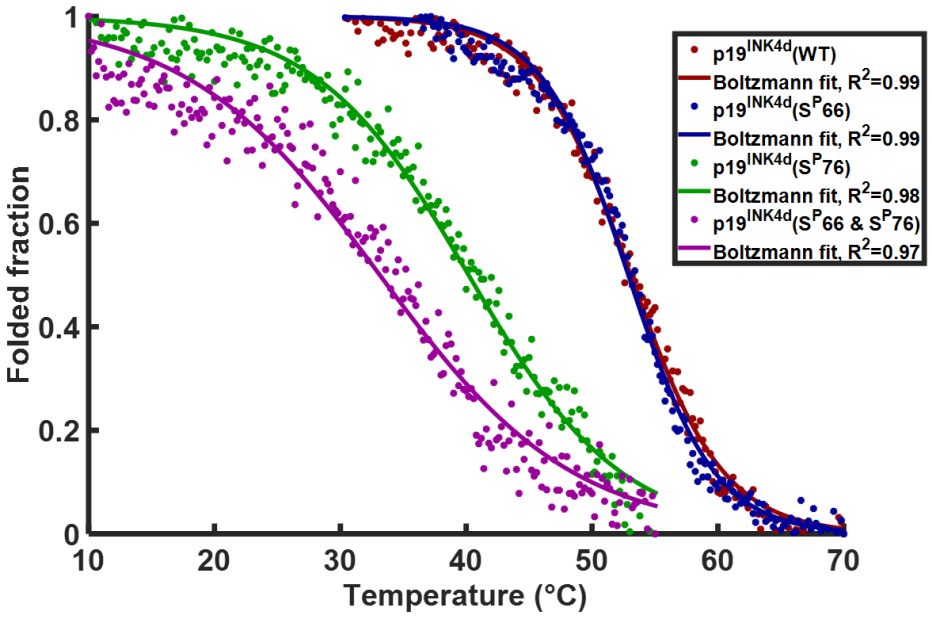

Figure S20. Folded fraction plotted against temperature, calculated using Boltzmann equation to fit the sigmoidal curves obtained from thermal scans at 208 nm (**Figure 3A**, main text). Concentrations determined were 9 μM for p19^{INK4d}(WT), 13 μM for p19^{INK4d}(S^{P}66), 10 μM for p19^{INK4d}(S^{P}76) and 10 μM for p19^{INK4d}(S^{P}66 & S^{P}76). Mean Tm values ± SD were calculated from 3 independent measurements for each p19^{INK4d} analogue where Tm_{208nm} for p19^{INK4d}(WT) = 52 ºC ± 1, Tm_{208nm} for p19^{INK4d}(S^{P}66) = 52 ºC ± 1, Tm_{208nm} for p19^{INK4d}(S^{P}76) = 42 ºC ±1 and Tm_{208nm} for p19^{INK4d}(S^{P}66 & S^{P}76) = 35 ºC ± 1.

Repetitive measurements

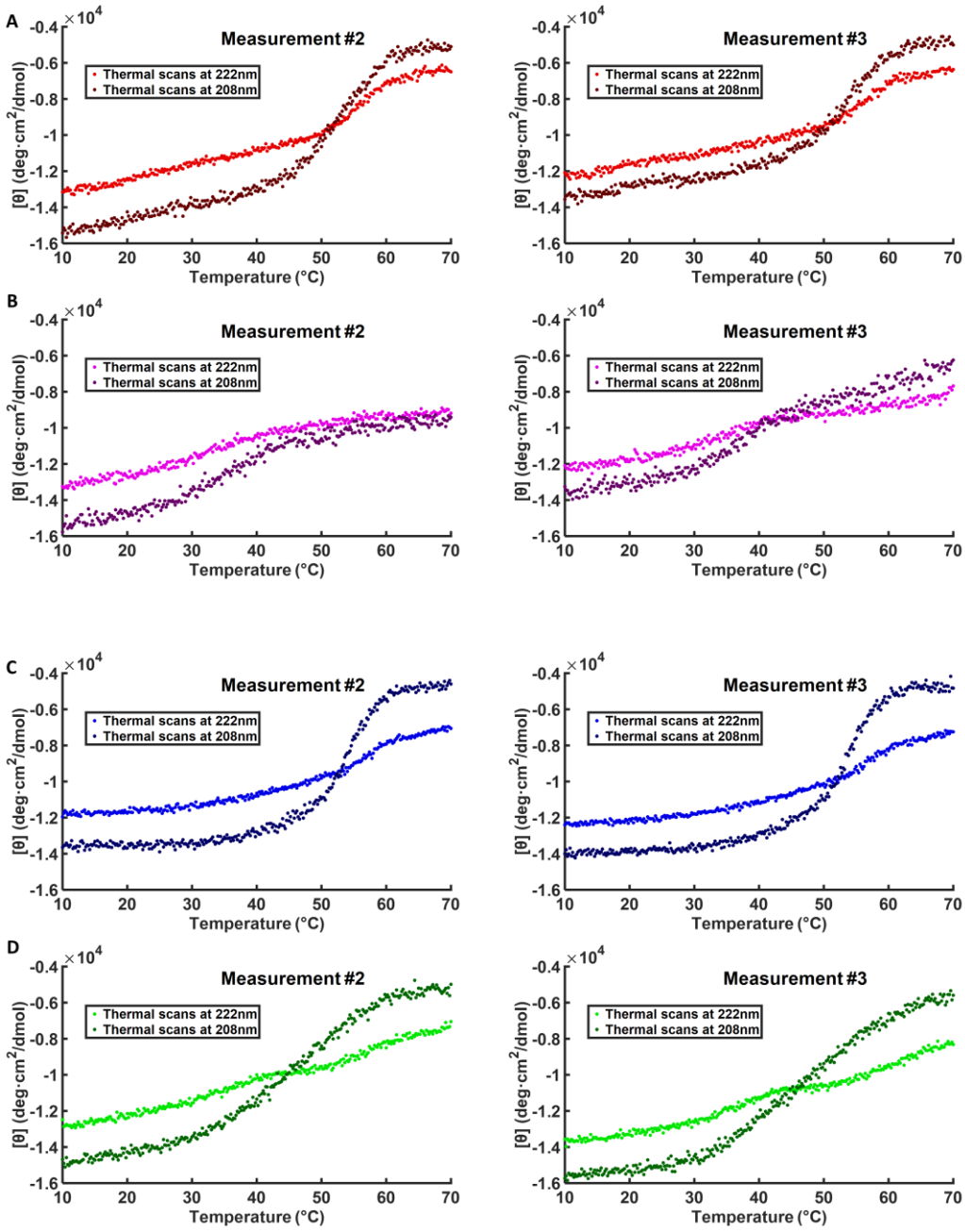

Figure S21. Two separate repeated measurements (measurement #2 & #3) of thermal scans from 10 ºC to 70 ºC obtained for all the analogues of $p19^{INK4d}$ at 222 nm and 208 nm wavelength used to calculate the average Tm; red-$p19^{INK4d}$(WT), purple-$p19^{INK4d}$(S^P66 & S^P76), blue-$p19^{INK4d}$(S^P66), green-$p19^{INK4d}$(S^P76). Concentrations determined for measurement #2 and measurement #3 are 11 µM and 12 µM for $p19^{INK4d}$(WT), 9 µM and

7 μM for p19^{INK4d}(S^{P}66 & S^{P}76), 16 μM and 15 μM for p19^{INK4d}(S^{P}66), and 13 μM and 14 μM for p19^{INK4d}(S^{P}76), respectively.

23. H-D exchange experiments

From the stock solution made for CD measurements, 2 μL of each analogue in Gn·HCl was taken and rapidly folded by adding 50 mM sodium phosphate in 25 % glycerol, pH = 7.4 to a final volume of 100 μL (2% 6 M Gn·HCl). The folded solutions were spun down, and the clear solutions were collected, and left on ice for 90 min. For control, each analogue was collected using HPLC with a gradient of 0-95 % B in 12 min where A is TFA at a pH~2.5 and B is acetonitrile at a pH~ 2.5. 10-fold buffer of 50 mM sodium phosphate, 25 % glycerol in D_2O, pH = 7.4 was added to the first tested analogue, left for 5 min in room temperature then directly injected and collected using HPLC with the same gradient stated above. The desalted sample was immediately checked using ESI-MS spectroscopy, followed by the corresponding control analogue. This procedure was repeated for the rest of the tested analogues. For p19^{INK4d}(S^{P}66) and p19^{INK4d}(S^{P}76) analogues, additional samples were checked after 21 h in 4 ºC.

We observed H-D exchange for all the analogues with a higher exchange rate for the **p19^{INK4d}(S^{P}76)** and the **p19^{INK4d}(S^{P}66 & S^{P}76**) analogues (17.6 ± 5.7 Da and 16.1 ± 4.8 Da respectively) after 5 min indicating the similarity of their structures compared with **p19^{INK4d}(S^{P}66)** analogue that showed similar exchange rate to **p19^{INK4d}(WT)** analogue (10.3 ± 4.2 Da and 8.5 ± 5.8 Da respectively). After incubation for 21 h at 4 ºC the difference in Da was still higher for **p19^{INK4d}(S^{P}76)** than for **p19^{INK4d}(S^{P}66)** (18.4 ± 4.2 and 13.4 ± 3.8 Da respectively).

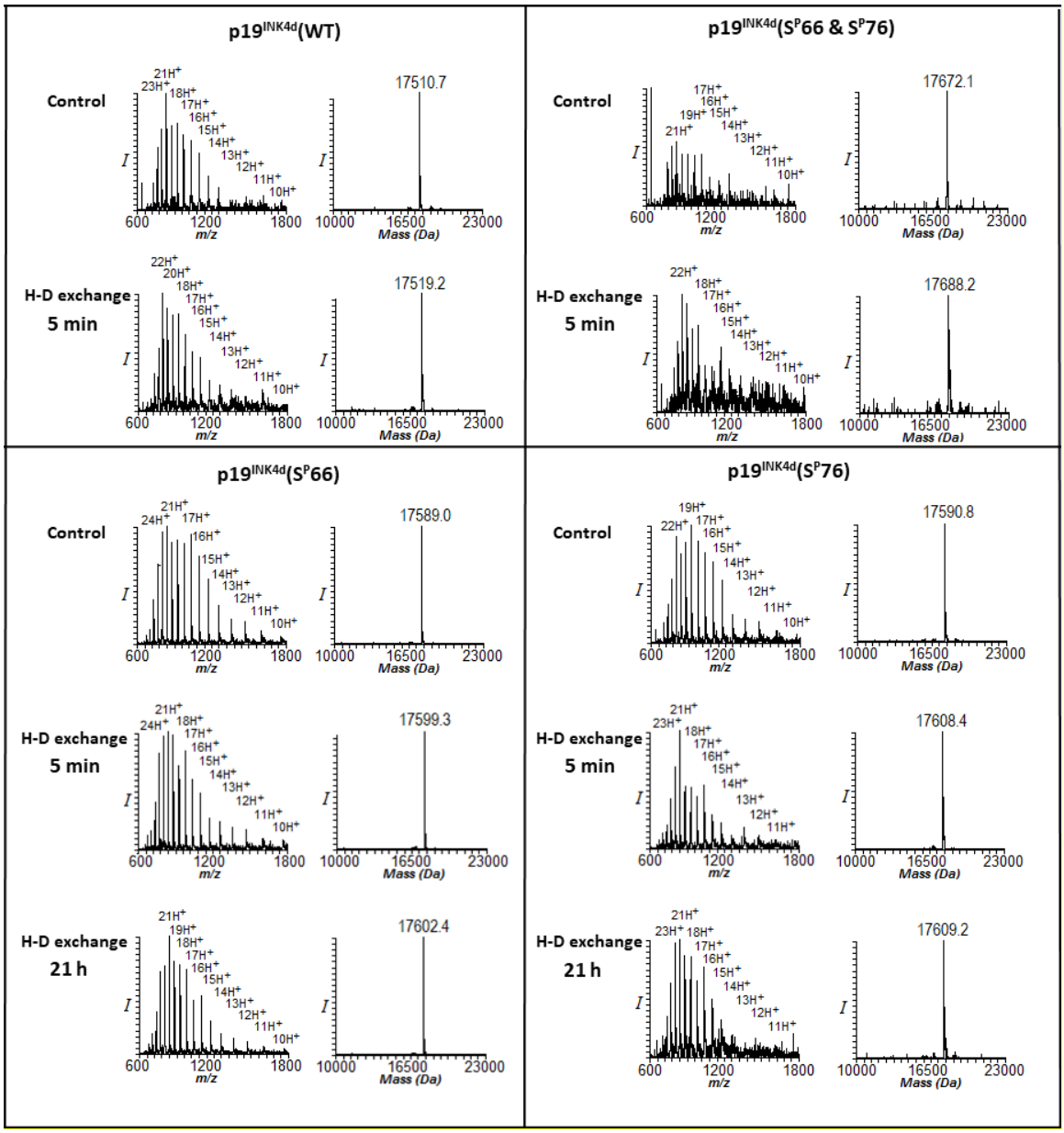

Figure S22. H-D exchange experiments for the examined analogues to determine structure changes upon different phosphorylation. For p19^{INK4d}(WT), the observed mass prior experiment was 17510.7 ± 4.8 Da, H-D exchange after 5 min showed an observed mass of 17519.2 ± 3.3 Da. For p19^{INK4d}(S^{P}66 & S^{P}76), the observed mass prior experiment was 17672.1 ± 2.1 Da, H-D exchange after 5 min showed an observed mass of 17688.2 ± 4.4 Da. For p19^{INK4d}(S^{P}66), the observed mass prior experiment was 17589.0 ± 1.6 Da, H-D exchange after 5 min showed an observed mass of 17599.3 ± 3.9 Da, H-D exchange after 21 h showed an observed mass of 17602.4 ± 3.5 Da. For p19^{INK4d}(S^{P}76), the observed mass prior experiment was 17590.8 ± 2.0 Da, H-D exchange after 5 min showed an observed

mass of 17608.4 ± 5.4 Da, H-D exchange after 21 h showed an observed mass of 17609.2 ± 3.7 Da.

24. In vitro ubiquitination assay

Hela cells were cultured and synchronized to S-phase with thymidine following the protocol used by reference (*Proc. Natl. Acad. Sci. U. S. A.*, **2018**, *115*, 3344–3349). Lysis was accomplished using freeze and thaw method using 5-7 cycles in DPBS buffer (Cat No. 02-020-1A) in the presence of protease (Cat No. 5391341ML; Merck Millipore) and phosphatase **(**PHOSS-RO; Sigma Aldrich) inhibitors. *In vitro* folded synthetic analogues (0.06 μg) were incubated at 37 ºC for 1 h (in a volume of 20 μL) in the presence of S-phase synchronized HeLa cell lysate (25 μg), Ub (15 μg), E1 (0.25 μg), E2 (1 μM), MG132 (3 μM), Ub aldehyde (Ubal; 5 μM) and ATP (7.5mM). Reactions were terminated by the addition of 5-fold concentrated sample buffer, and proteins were resolved via 10 % tris-tricine SDS-PAGE, then transferred to a membrane for western blot analysis where it was probed with an anti-HA-tag chip (ab9110) antibody and p19 Antibody (DCS-100) (sc-56334).

U2OS cells were synchronized using Hydroxyurea (HU), where cells were grown until 60 % density, then HU was added in 2mM concentration in medium and left for 20 h, then fresh medium was added and the cells were left for additional 3 h. Lysis for U2OS cells was done using 0.1 % NP-40 (Cas no. 9016-45-9, Merck Millipore), 10 % glycerol in DPBS buffer in the presence of protease and phosphatase inhibitors stated above. Ubiquitination assay was done as stated above with the addition of 375 nM from each p38 and CDK1 kinase inhibitors (SB 203580; Cas no. 152121-47-6, RO-3306 Cas. No 872573-93-8). proteins were resolved via 10 % tris-tricine SDS-PAGE or 10 % glycine SDS-page.

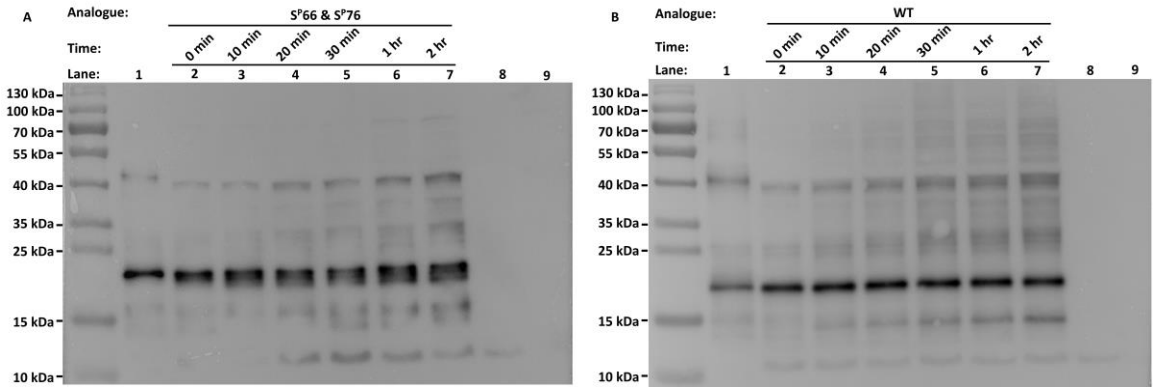

Figure S23. Time course Ubiquitination assay for $p19^{INK4d}(S^P66$ & $S^P76)$ and $p19^{INK4d}$(WT) analyzed without the addition of phosphatase and protease inhibitors. A) Lane 1 corresponds to the synthetic $p19^{INK4d}(S^P66$ & $S^P76)$ analogue for comparison. Lane 2-7 of the ubiquitination assay taken at different time points without the addition of phosphatase inhibitor showing the dephosphorylation of the analogue as indicated by the appearance of two lower bands. Lane 8 is lysate incubated for 2 h with all the compounds of ubiquitination assay for control. Lane 9 is lysate alone for additional control. Anti $p19^{INK4d}$ antibody was used to probe the western blot. B) Ubiquitination assay for $p19^{INK4d}$(WT). Lane 1 corresponds to the synthetic $p19^{INK4d}$(WT) analogue for comparison. Lane 2-7 of the ubiquitination assay taken at different time points without phosphatase inhibitors. Lane 8 is lysate incubated for 2 h with all the compounds of ubiquitination assay for control. Lane 9 is lysate alone for additional control. Anti $p19^{INK4d}$ antibody was used to probe the western blot.

Supporting ubiquitination assays:

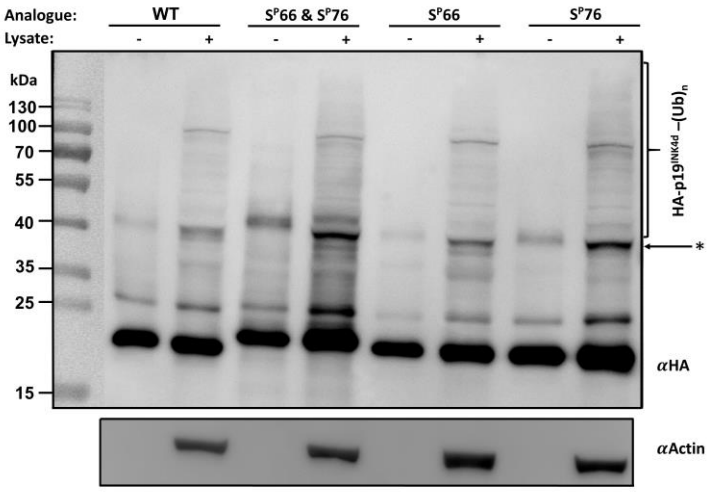

Figure S24. Ubiquitination study of HA-p19^{INK4d} analogues. Immunoblot of each synthetic analogue of HA-p19^{INK4d} with and without incubation in S-phase HeLa cell lysate is shown for comparison. The reactions were left for 1 h incubated at 37 ^{o}C. Actin is shown below as a loading control.

* Unidentified band at 40 kDa can correspond to impurity and poly-ubiquitinated p19^{INK4d}.

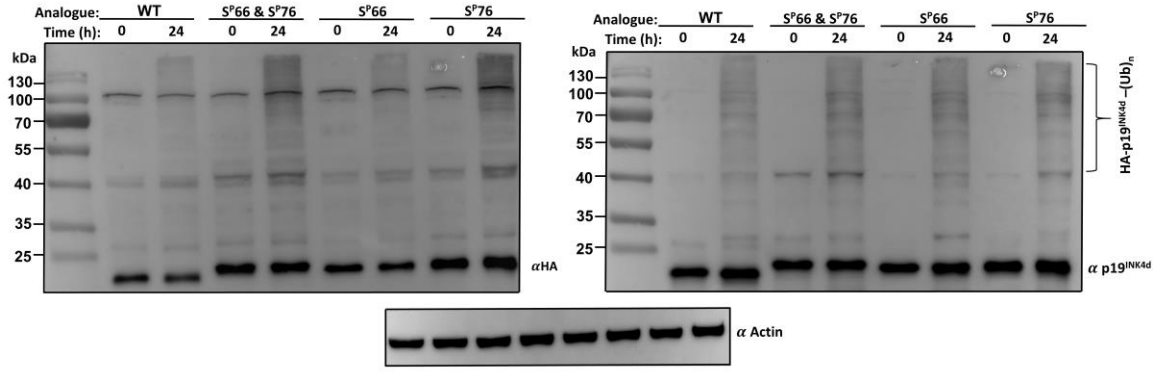

Figure S25. Immunoblot for additional *in vitro* ubiquitination assay with S-phase HeLa cell lysate and compounds stated above taken before incubation in 37 ^{o}C (0 h) and 24 h after incubation for each HA-synthetic analogue. The same membrane was blotted with anti HA, anti p19^{INK4d}, and anti actin antibodies.

Additional *in vitro* ubiquitination assays using U2OS cells:

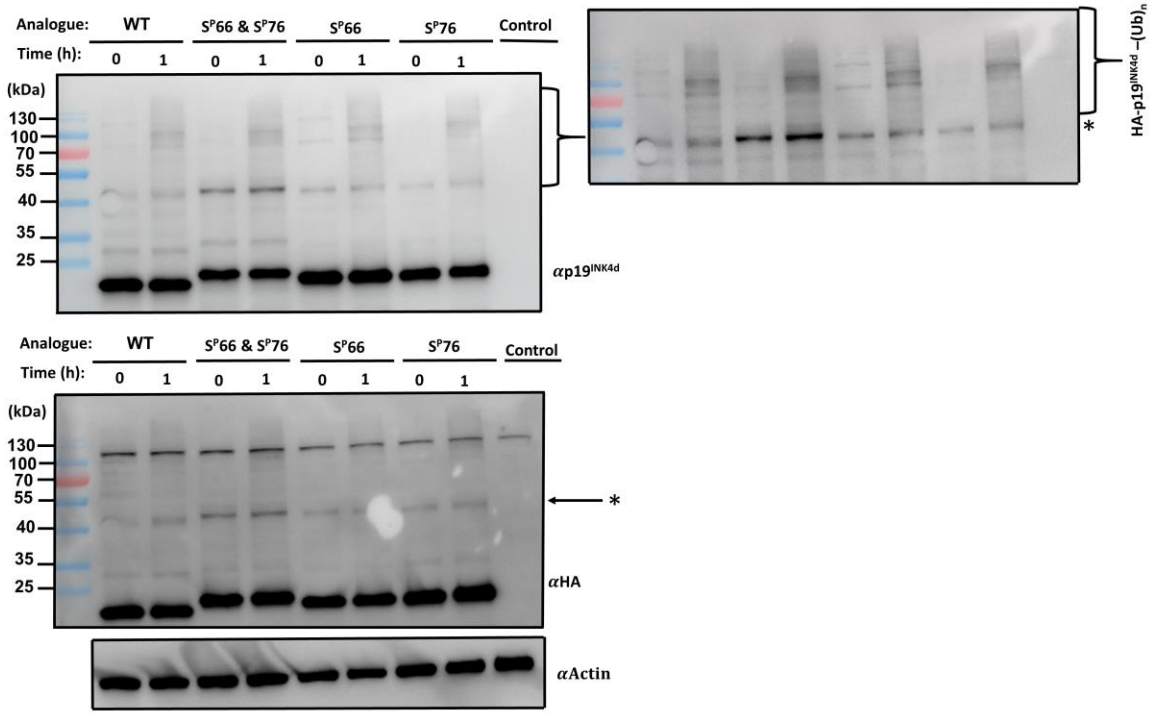

Figure S26. Immunoblot for additional *in vitro* ubiquitination assay with S-phase U2OS cell lysate and compounds stated above taken before incubation in 37 ^{o}C (0 h) and 1 h after incubation for each HA-synthetic analogue. Control contained assay compounds with cell lysate. The same membrane was blotted with anti HA, anti p19^{INK4d}, and anti actin antibodies. In comparison with HA-p19^{INK4d}(WT), polyubiquitination of HA-p19^{INK4d}(S^{P}66 & S^{P}76) and HA-p19^{INK4d}(S^{P}66) increased by 39 % and 6 % respectively while HA-p19^{INK4d}(S^{P}76) was reduced by 11 %.

* Unidentified band at 40 kDa can correspond to impurity and poly-ubiquitinated p19^{INK4d}.

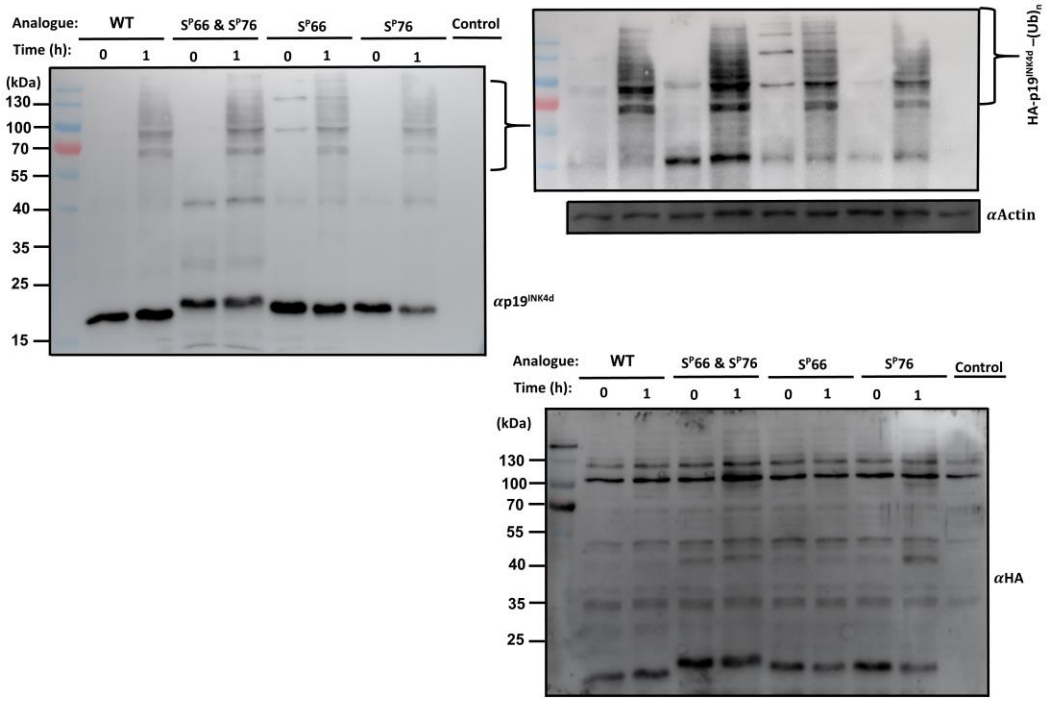

Figure S27. Immunoblot for additional *in vitro* ubiquitination assay with Abcam's Ubiquitylation Assay Kit- HeLa lysate-based (ab139471). The experiment was done according to the suggested Kit assay protocol with the addition of phosphatase inhibitors, p38 and CDK1 kinase inhibitors (375 nM), MG132 proteasome inhibitor (5 μM), 100 mM creatine phosphate and 2 μg/ml creatine phosphokinase. Reaction were taken at 0 h and 1 h after incubation for each HA-synthetic analogue and were resolved on a 10 % tris-glycine SDS page. Control contained assay compounds without the tested analogues. The same membrane was blotted with anti HA, anti $p19^{INK4d}$, and anti-actin antibodies. HA-$p19^{INK4d}$(S^P66 & S^P76) showed the highest ubiquitination signal.

Verification of stepwise phosphorylation confirming the suggested mechanism by Balbach group:

p19^{INK4d}(WT) and p19^{INK4d}(S^{P}66) (600 ng) analogues were incubated in 37 ^{o}C each with ATP (10 µM), cAMP (10 µM) and CDK1/cyclinB (250 ng, 300 nm) in 6µl 10% glycerol DPBS buffer. 3 µl was taken after the addition of all the compounds before incubation in 37 ^{o}C (0 h) and 4 h after incubation in 37 ^{o}C and resolved on 16 % tris-tricine gel (Figure S27). The stepwise phosphorylation proposed by Balbach group, which suggested that phosphorylation on Ser76 using CDK1/cyclinB only occurs when Ser66 is phosphorylated (using p38 Kinase) was confirmed. while two bands were detected after 4 h for HA-p19^{INK4d}(S^{P}66) indicating the phosphorylation of this analogue using CDK1/cyclinB kinase, no additional band was detected for the HA-p19^{INK4d}(WT) analogue.

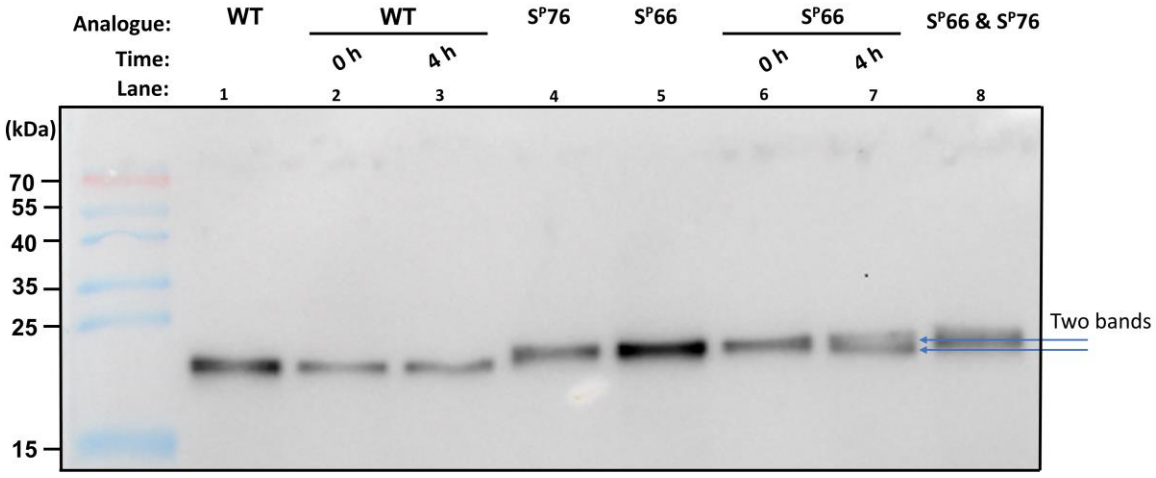

Figure S28. Kinase assay for HA-p19^{INK4d}(WT) and HA-p19^{INK4d}(S^{P}66). Lane 1,4,5,8 are the four different analogues resolved for comparison and control. Lane 2,3 and lane 6,7 are the kinase assay incubated with CDK1/cyclinB for HA-p19^{INK4d}(WT) and HA-p19^{INK4d}(S^{P}66) analogues, respectively. The membrane was probed with anti-HA antibody.